HYDROGRAPH SEPARATION USING HYDROCHEMISTRY MIXING MODELS:
An assessment of the Langtang River Basin, Nepal

By Alāna M Wilson

B.S. Geological Sciences
University of North Carolina at Chapel Hill (2008)

A Thesis submitted to the
Faculty of the Graduate School of the
University of Colorado in partial fulfillment
of the requirement for the degree of
Master of Arts
Department of Geography 2015

This thesis entitled:
Hydrograph Separation Using Hydrochemistry Mixing Models:
An assessment of the Langtang River Basin, Nepal
written by Alāna M. Wilson
has been approved for the Department of Geography

_____
Mark W. Williams

_____
Richard Armstrong

_____
Peter Blanken

*Date*_____

The final copy of this thesis has been examined by the signatories, and we
Find that both the content and the form meet acceptable presentation standards
Of scholarly work in the above mentioned discipline.

ABSTRACT

Wilson, Alāna M. (M.A., Geography)

Hydrograph Separation Using Hydrochemistry Mixing Models: An assessment of the Langtang River Basin, Nepal

Thesis directed by Professor Mark W. Williams

While there have been increased efforts recently to understand the dynamics of Asia's cryosphere, glacier melt dynamics and hydrograph separation of river discharge are open questions. A multi-year, multi-seasonal data set of water chemistry from the Langtang Valley, Nepal is used to explore source waters and flow paths that contribute to Langtang River discharge. Bulk monsoon precipitation samples from the Langtang Valley shows a linear relationship of 2.3‰ depletion of the oxygen-18 isotope per kilometer of elevation gain. Differences in hydrochemistry of samples from the clean-ice Khimsung Glacier and debris-covered Lirung Glacier suggest that debris-cover can induce more melt-freeze cycles in glacier ice and can elevate the concentrations of geochemical weathering products in glacier outflow. Additional data shows seasonal transitions in the composition of Langtang River discharge Two-component mixing models using melt water and groundwater oxygen-18 values are sufficient to explain October 2008 and November 2013 Langtang River water samples, but a combination of rain/snow and melt water oxygen-18 isotope values are required to explain May 2012 Langtang River water samples. End Member Mixing Analysis (EMMA) using geochemical and isotopic tracers suggests reacted meltwater contributes the majority of flow in late fall, while the proportion of unreacted meltwater increases during the late spring and early fall – the shoulder seasons of the monsoon. We hypothesize our data set is missing characteristic monsoon water and utilize a late May Langtang River water sample as a proxy for monsoon-influenced groundwater in the EMMA. Results offer insight into the plausibility of flow sources and pathways in the basin.

ACKNOWLEDGEMENTS

Many thanks to Mark Williams for his support, guidance, and insight throughout the many iterations of this process. I also greatly appreciate the feedback and suggestions of committee members Richard Armstrong and Peter Blanken. Thanks to Rijan Kayastha of Kathmandu University for his vision to expand glaciological research in Nepal and the Langtang Valley. Thanks to ICIMOD for assisting in coordination of field logistics, and to Inge Juszak and ETH Zürich for automatic sampling equipment and collection. Financial support for this research came from USAID Cooperative Agreement AID-OAA-A-11-00045, a National Aeronautics and Space Administration Earth and Space Science Fellowship and the University of Colorado Department of Geography Adam Kolff Memorial Scholarship.

Table of Contents

1. Overview 1
1.1 The cryosphere and melt 1
1.2 Hydrologic mixing models 4
2. Field Area 6
3. Methods 13
3.1 Sample collection 13
3.2 Laboratory Analysis 16
3.3 Hydrologic mixing models 17
3.4 Two-component mixing models 19
3.5 End Member Mixing Analysis 20
4. Results and Discussion 24
4.1 Chemistry and Isotopic Tracers 24
4.2 Diurnal behavior of clean-ice and debris-covered glaciers 30
4.3 Langtang River hydrograph Separation 35
4.3.1 Mixing models 35
4.3.2 End Member Mixing Analysis (EMMA) 36
5. Conclusions 47

List of Tables

Table 1. Results of studies which have calculated basin area and glacierized area in the Langtang Valley. The three studies used the same pour point to define the Upper Langtang Basin 7

Table 2. Locations and timing of Langtang River water and its end members, and median values of oxygen-18 isotope data 14

Table 3. Two-component mixing model results for three years of Langtang River water samples 35

Table 4. Principal Component Analysis results for the Langtang River samples using seven tracers. 38

Table 5. EMMA results for all Langtang River water samples 42

List of Figures

Figure 1. Overview of Langtang Valley location in the Nepalese Himalayas and sampling locations 6

Figure 2. Lirung sub-basin sampling locations 8

Figure 3. (a) View from lateral moraine east across debris-covered tongue of Lirung Glacier, with Khimsung Glacier's clean-ice terminus in the background. (b) Down-glacier (south-facing) view from Lirung Glacier debris-covered terminus; terminal moraine lake is ~1 km in length and lateral moraines estimated at ~20 – 30 m in height (photos: A. Wilson) 8

Figure 4. Runoff and precipitation patterns in the Upper Langtang Valley both averaged from 1998-2006: (a) daily discharge at the DHM Gauge; (b) monthly precipitation pattern as measured at Kyangjing station (from Racoviteanu et al., 2013) 9

Figure 5. Daily precipitation (bars) and hourly temperature (grey line) at 4831 m station in Langtang Valley between May 2012 and May 2013. Vertical dotted line delineates seasons (from Immerzeel et al., 2014) 10

Figure 6. Monthly precipitation in 2012 at different elevations in the Langtang Valley, Nepal (from Baral et al., 2014) 11

Figure 7. Energy fluxes at an ice cliff surface in the ablation zone of Lirung Glacier from 25 April – 22 October 1996, where I = net shortwave radiation, R = net longwave radiation, H = turbulent sensible heat flux, E = turbulent latent heat flux (from Sakai et al., 1998) 12

Figure 8. Mixing equations and visualization for two end member mixing model (Vaughn, 1994) 19

Figure 9. Four end members with two-dimensional mixing space determined by PCA; where the black dots (original End Member) have been re-projected into the 2D plane (white rectangle) and 3 of them will be chosen as the end member contributors to the composition of samples in the striped data cloud (from Christophersen and Hooper, 1992) 21

Figure 10. Boxplots comparing pre-monsoon (May 2012) and post-monsoon (October/November 2013) values of geochemical and isotopic tracers in Langtang river water and its end members: rain (rn), snow (sn), groundwater (gw), melt stream (ms), Khimsung Glacier (Km), Lirung Glacier (Li), Lirung Glacier Ice (LiI), Lirung Moraine (LiM), Lirung Supraglacial (LiS), Langtang Glacier (Lng), Langtang Glacier Ice (LngI), Langshisha Glacier (Lsh), Yala Stream (YaS) 25

Figure 11. Langtang River water samples relative to the Global Meteoric Water Line 27

Figure 12. Isotopic gradient of 2012 monsoon precipitation in the Langtang Valley 29

Figure 13. Monthly variations of the weighted mean δ18O and precipitation at Kyangjing from May, 1993 to October, 1996. (Zhang, 2001) 30

Figure 14. Isotopic trends for bihourly sampling at the clean-ice Khimsung Glacier and the debris-covered Lirung Glacier in May 2012 32

Figure 15. Select geochemical tracer trends for bihourly sampling at the clean-ice Khimsung Glacier and the debris-covered Lirung Glacier in May 2012. Vertical dashed lines mark noon for each day 34

Figure 16. Trends in Langtang River water chemistry by season 37

Figure 17. EMMA results for three seasons of Langtang Valley water samples. Where: rain (rn), snow (sn), groundwater (gw), melt stream (ms), Khimsung Glacier (Km), Lirung Glacier (Li), Lirung Glacier Ice (LiI), Lirung Moraine (LiM), Lirung Supraglacial (LiS), Langtang Glacier (Lng), Langtang Glacier Ice (LngI), Langshisha Glacier (Lsh), Yala Stream (YaS) 41

Figure 18. Tracer concentrations (µeq l-1) predicted using two Principal Components versus tracer concentrations measured in each Langtang River sample 45

Figure 19. Biplot of Principal Component 1 and Principal Component 2 46

1. Overview

1.1 The cryosphere and melt

Mountains, the 'water towers of the world' (Bandyopadhyay et al. 1997), play an invaluable role in regulating the hydrologic resources that downstream communities depend on. Many of our societies are adapted to a water cycle that includes the storage of water at high elevations as ice and snow until spring and summer temperatures release it as meltwater for use in irrigation, hydropower, and for commercial and municipal purposes (Williams et al. 2011). The role of mountain snow/ice storage in providing downstream water supplies is significant around the globe, particularly in arid regions and in some basins with large populations. For example, more than 90% of water in the Indus River Basin originates in mountainous terrain (Messerli et al., 2004). As our climate changes, it is essential that we evaluate the vulnerability of the high-elevation water cycle and the water resources that depend on it (Xu et al., 2009). An improved understanding of where the water in our rivers comes from is required, before we can anticipate changes and devise adaptation measures. Thapa (1992) discussed the "urgency of snow hydrology" for successfully understanding water resources in the Himalayan region. Along with evaluating the role of glacier melt in alpine hydrology, that urgency remains today.

Snow and glaciers of High Mountain Asia are the source of water for much of the continent's population (Immerzeel et al., 2010). In South Asia, monsoon activity strongly influences the timing of precipitation, as well as the energy balance of glaciers and snowpack (Sakai et al., 1998; Baral et al., 2014). An additional complication is that debris cover can be extensive on glacier tongues and enhance or inhibit melt, depending on thickness (Kayastha, 2000). Water balance, the net movement of water in or out of a system, requires numerous input and output parameters that are often difficult to quantify at the basin scale. The remote and rugged

terrain of the Himalayas make it a data-poor region with respect to traditional ground-based glaciological (UNEP & WGMS, 2008) and hydrometeorological (Chalise et al, 2003) measurements. Remote sensing faces several challenges closing the water balance, and even on the ground, field measurements may not be representative or accurate when extrapolated (Zemp et al., 2009; Nepal, 2014). Hydrochemistry-based mixing models offer an alternative by utilizing naturally occurring tracers to estimate proportions of river discharge from various sources and flow paths.

The Himalayan region is of particular interest in efforts to understand the impacts of climate change and rising temperatures on the terrestrial cryosphere (Bolch et al., 2012; Kargel et al., 2011; Immerzeel et al., 2010). The degree of variability in published assessments quantifying snow and ice melt has resulted in a high amount of uncertainty regarding the vulnerability of the region in the face of a warming climate (Armstrong, 2011). Problematic estimates of the contribution of meltwater to discharge of major South Asian rivers include the assertion in Barnett et al. (2005) that summer flow in the Ganges is comprised of as much as 70% glacier melt. They, however, fail to acknowledge the potential convolution of snow melt and ice melt, and the difficult-to-quantify combination of snow melt and ice melt that comprise outflow at a glacier's terminus. Such high values have been contradicted (Kaser et al., 2010) and the associated alarmist messaging has been criticized (Miller et al., 2012). Other studies have acknowledged the inability to distinguish between glacier melt and snow melt (Bookhagen and Burbank, 2010). Separating the melt of seasonal snow from glacial ice is fundamental since snow is a water resource that is re-supplied each year in varying quantities. Changes in alpine hydrology are expected as snow and ice are subjected to an estimated temperature increase of 0.06 ^{o}C/yr in the Himalayan mountain region over the rest of this century due to climate change (Immerzeel et al, 2012).

As glaciers retreat and precipitation changes from snow to rain, the hydrographs in snow and ice-covered catchments will change. Glacierized catchments like the Langtang Valley of Nepal have the potential to transition to a snowmelt and monsoon dominated hydrograph, which could reduce peak discharge in late summer relative to present trends influenced by late-summer glacier melt (Immerzeel et al., 2012). For downstream water users, understanding shifts in the hydrograph has profound implications for management.

The chemistry of water as it moves through a catchment provides information on its sources and subsequent pathways. Measurement of geochemical species in water samples differentiates them into two primary categories: "reacted" waters and "unreacted" waters (Sueker et al., 2001). Reacted waters typically travel in the subsurface and acquire elevated solute levels via ion exchange or mineral weathering. In glacierized catchments this increase in concentration of chemical tracers commonly happens with flow through moraines or glacial till, and depends on length of contact with solute sources. Surface waters that have not undergone any infiltration, such as some snow melt and glacier ice melt, typically have low solute concentrations and are considered unreacted waters.

Isotopic tracers, in contrast to geochemical tracers, are not influenced by flow path unless evaporation occurs, but they can potentially provide useful information on the location or timing of the original precipitation source (Hooper & Shoemaker, 1986). The oxygen-18 isotope in water is known to become more depleted with colder temperatures, higher elevations, and distance from moisture source (Poage & Chamberlain, 2001). This affects the seasonal variability of isotope values.

1.2 Hydrologic mixing models

Hydrologic mixing models have a long history of application in catchments where water chemistry data are available (e.g. Johnsen et al., 1969; Sklash et al, 1976; Robson & Neal, 1990). Hydrologic mixing models are a form of hydrograph separation - the differentiation of end member source waters that contribute to river discharge (e.g. Hooper and Shoemaker, 1986; Wels et al., 1991; and Hoeg et al., 2000); end members being the sources that add up to total streamflow. Hydrologic mixing models utilize the unique geochemical and isotopic chemistry of different end member sources to quantify their contribution to discharge in a catchment (e.g. snow melt, glacier melt, groundwater, rain). Discharge data is not required as the hydrograph separation estimates proportionate contributions that come from each end member (Liu et al., 2004), which makes them particularly strategic for poorly-monitored glacierized catchments (Barthold et al., 2010). Discharge data in glacierized basins is often difficult to obtain due to inaccessibility and the fact that channel cross-section instability makes rating curves for stage height unreliable (Nepal, 2014). Mixing model results may also provide insight into how the timing and volume of discharge could change in response to changes in climate (Kong and Pang, 2012).

Hydrologic mixing models have not been applied extensively in Himalayan catchments and literature on the topic largely deals with paths of geothermal waters (e.g. Giggenbach et al., 1983), chemical denudation rates (e.g. Hodson et al., 2002), and geographic sources of precipitation (e.g. Karim & Veizer, 2002). The only applications of mixing models to quantify meltwater that we know of in the monsoon-influenced central Himalayas are: Lambs (2000), Maurya et al. (2011), and Racoviteanu et al. (2013). Lambs (2000) separated ice melt from snow melt in streamwater in the headwaters of the River Ganga based on isotopic and conductivity values, but did not consider the role of groundwater. Maurya et al. (2011) quantified the time-

varying relative fraction of end members in the River Ganga at an elevation of 372 m using fortnightly samples over the course of 18 months. However they did not attempt to differentiate liquid precipitation from snowmelt. Racoviteanu et al. (2013) demonstrated that utilizing $\delta^{18}O$ as the sole tracer in post-monsoon conditions produces plausible results separating groundwater from snow and ice melt in the Langtang River basin, results which are comparable to estimates they found using an elevation-dependent ice ablation model derived from remote sensing data.

An improvement on the hydrologic mixing model is the End Member Mixing Analysis (EMMA) presented in Christophersen et al., 1990 and Hooper et al., 1990. EMMA allows for the inclusion of an unlimited number of geochemical and isotopic tracers by reducing the dimensionality of the data with Principal Component Analysis (PCA). EMMA also allows for consideration of all end members for which the user has chemistry data by plotting their chemistry relative to streamwater and using a least-squares method to select for those that best explain streamwater chemistry. While there is subjectivity involved, EMMA offers error analysis (e.g. proportion of variance explained) to better ensure that hydrograph separation produces the right answers for the right reasons. It does this by explicitly considering all end members which could potentially contribute to discharge and quantifying the percent relative error between the streamwater and the combination of end members that best explains the streamwater chemistry. EMMA has been utilized to examine rock glacier outflow (Williams et al. 2006), but we do not know of any applications in glacierized catchments.

This work is an evaluation of different hydrochemistry approaches to hydrograph separation and a contribution to defining the early 21st century baseline behavior of the Langtang River Basin, Nepal. Our attempts to identify source waters and flow paths are a contribution to understanding the vulnerability of the hydrograph to shifts in the timing of melt. The objective is

to distinguish potential end members through hydrograph separation and show that using hydrochemistry data for EMMA is potentially an appropriate tool to do this.

2. Field Area

Field work was conducted in the Langtang Valley of Nepal's central-eastern Himalaya (Figure 1), part of Langtang National Park approximately 60 km north of Kathmandu. The basin is defined upstream of the confluence of the Langtang River and Trishuli River, at 1460 m at the town of Syafrubensi. The highest point is Langtang Lirung's 7246 m summit. The Langtang Basin is in the headwaters of the Trishuli Basin, which flows into the Narayani Basin, a tributary of the River Ganga. The basin is 585 km^2 and at least 23% glacierized (from Motoyama and Yamada, 1989).

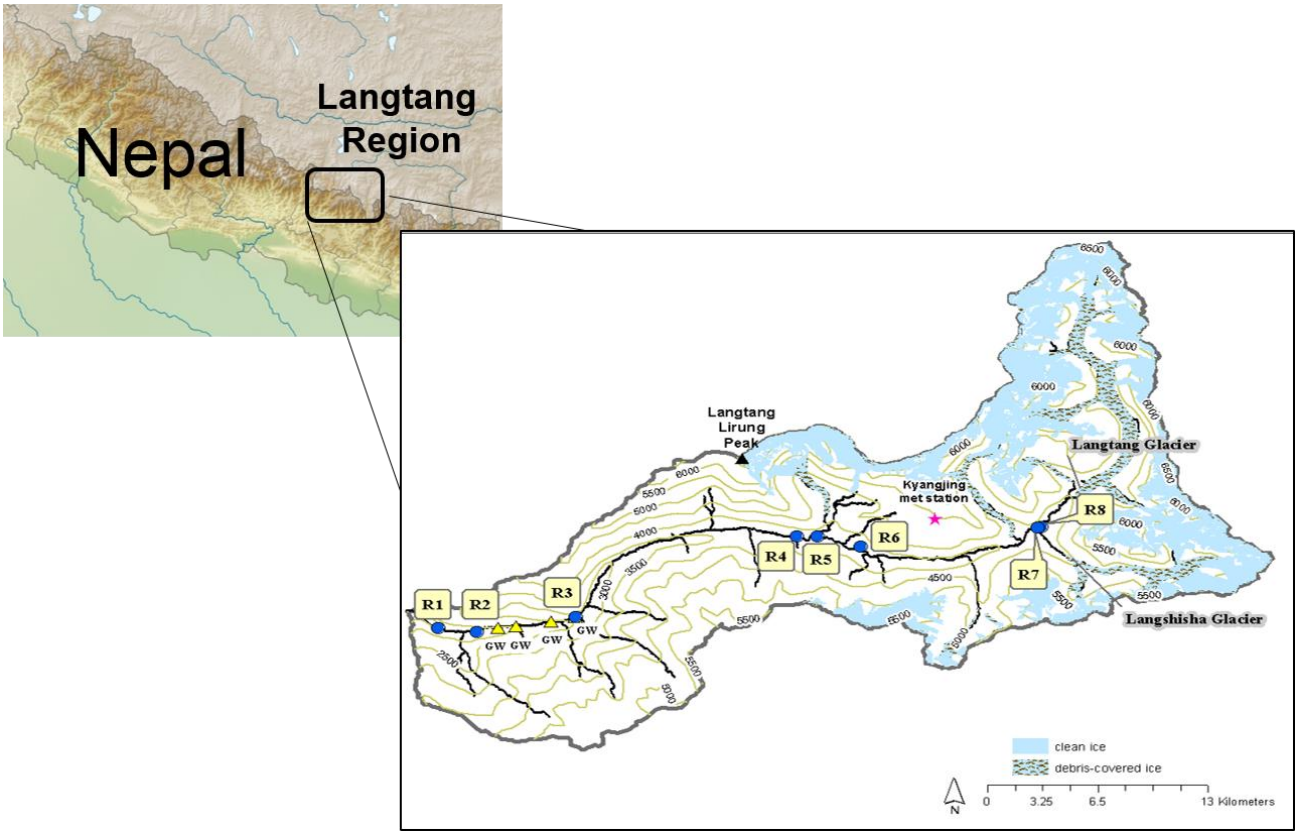

Figure 1. Overview of Langtang Valley location in the Nepalese Himalayas and sampling locations

The Upper Langtang Basin is defined upstream of the Nepali Department of Hydrology and Meteorology (DHM) gauging station at 3642 m (R4 in Figure 1). The Upper Langtang Basin (~350 km^2) is glacierized over a significant portion of its area. Ice-covered area estimates include 38%, 43.5%, and 46% (Motoyama and Yamada, 1989; Racoviteanu et al., 2013; Immerzeel et al., 2012) (Table 1). The Upper Langtang Basin includes the Langtang Glacier, which at ~75 km^2 (Wagnon et al., 2007) is the largest glacier in the catchment, as well as the main drainage for the Yala Glacier. The Langshisha Glacier (area >15 km^2) also contributes to streamflow in the Upper Langtang Basin.

Table 1. Results of studies which have calculated basin area and glacierized area in the Langtang Valley. The three studies used the same pour point to define the Upper Langtang Basin

Study	Basin	Calculated basin area (km^2)	Calculated glacier area within basin (%)
Motoyama & Yamada (1989)	Lirung sub-basin	13.8	45%
Motoyama & Yamada (1989)	Upper Langtang	333	38%
Immerzeel et al. (2012)	Upper Langtang	360	46%
Racoviteanu et al. (2013)	Upper Langtang	352.3	43.5%

The Lirung sub-basin (Figure 2), where much of the sampling was conducted, includes the debris-covered Lirung Glacier (7.2 km^2, Nakawo & Rana, 1999), the clean-ice Khimsung Glacier (4.23 km^2 in 1992, Kaufmann et al., 2013), and a drainage from the western section of the clean-ice Yala Glacier, an ice cap type glacier of less than 2 km^2 (Fujita & Takayuki, 2011). Based on May 2012 field observations, debris on the Lirung Glacier covers >90% of the bottom 3.5 km length of the tongue, which is separated from the accumulation area by an icefall. The debris consists of boulders up to 4 m in diameter and primary size classification is 0.5 to 1.0 m in diameter (Figure 3a). The debris is material largely sourced from the lateral moraines which now tower 20 m to 30 m above the glacier surface (Figure 3).

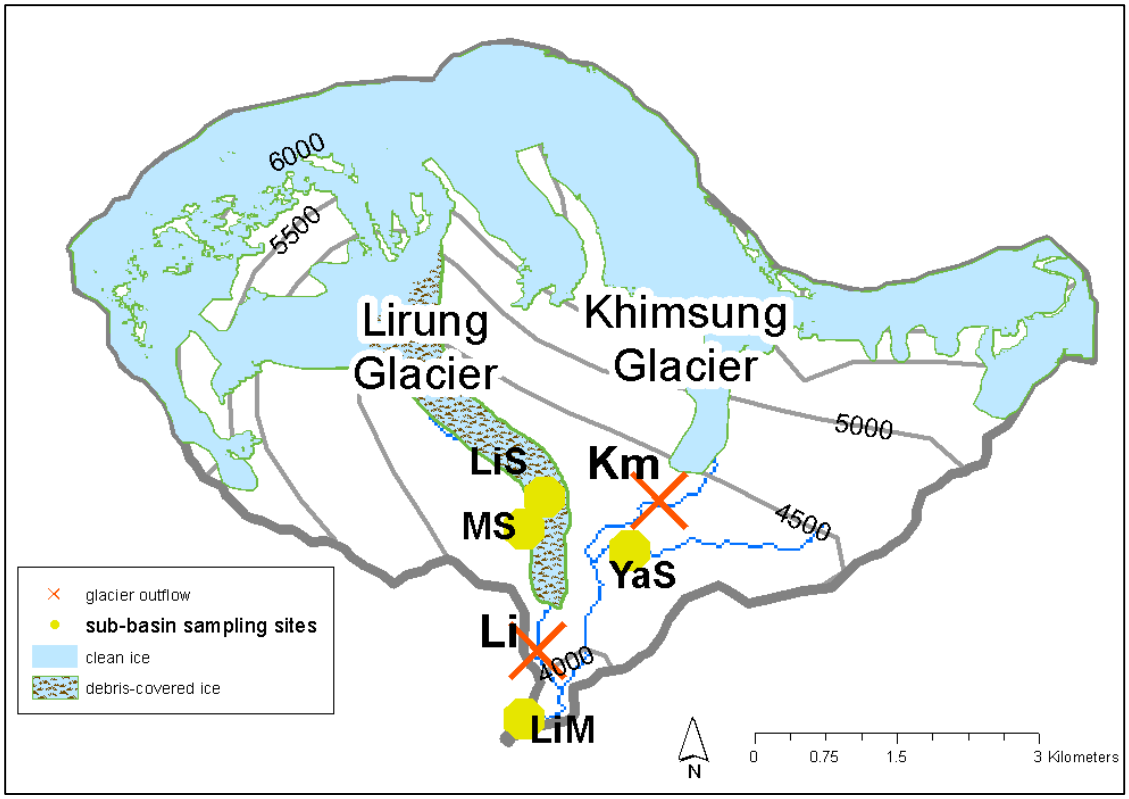

Figure 2. Lirung sub-basin sampling locations

Figure 3. (a) View from lateral moraine east across debris-covered tongue of Lirung Glacier, with Khimsung Glacier's clean-ice terminus in the background. (b) Down-glacier (south-facing) view from Lirung Glacier debris-covered terminus; terminal moraine lake is ~1 km in length and lateral moraines estimated at ~20 – 30 m in height (photos: A. Wilson)

Gauging station data from the DHM Gauge indicates flow out of the upper catchment ranges from 3 m^3/sec^1 to 16 m^3/sec^1 throughout the year (Racoviteanu et al., 2013; Figure 4a), and peaks during the summer monsoon. Annual precipitation measured by DHM averages 622 mm precipitation per year at the Kyangjing meteorological station (3924 m) with ~73% falling between May and September (Racoviteanu et al., 2013; Figure 4b). Barnard et al. (2006) reported the Equilibrium Line Altitude (ELA) of the valley to be 5320 m indicating that a large portion of the Upper Langtang Basin receives monsoon precipitation in the form of snow, contributing to the long-term survival of its glaciers.

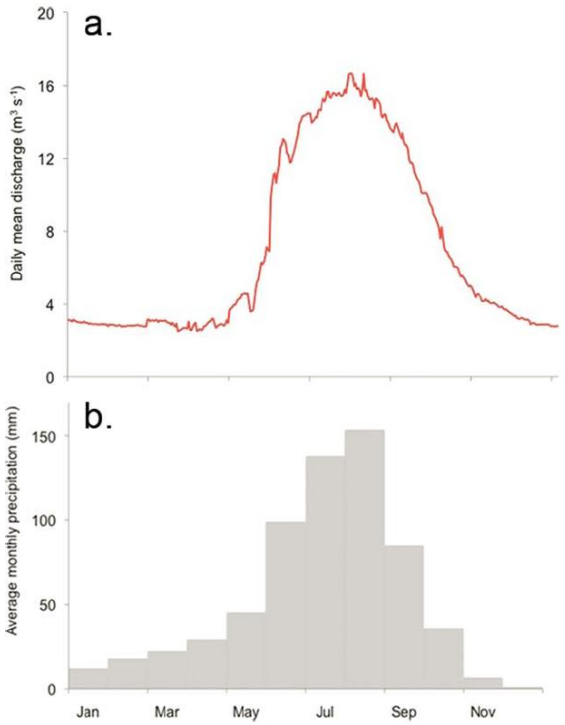

Figure 4. Runoff and precipitation patterns in the Upper Langtang Valley both averaged from 1998-2006: (a) daily discharge at the DHM Gauge; (b) monthly precipitation pattern as measured at Kyangjing station (from Racoviteanu et al., 2013)

Regional variability in monsoon precipitation volume is not well studied at the catchment scale, since spatial distribution is highly complex and affected by topographic controls (Kansakar, 2004). Recent work in the Langtang Valley has tried to address this knowledge gap. Immerzeel

et al. (2014) have published temperature and precipitation data from May 2012 – May 2013 (covering the May 2012 time period of this study) from a station at 4831 m (Figure 5). That station, demonstrates that most precipitation falls during the monsoon, but minimum temperatures are above freezing. Average annual temperature at this site however is -1.8° C.

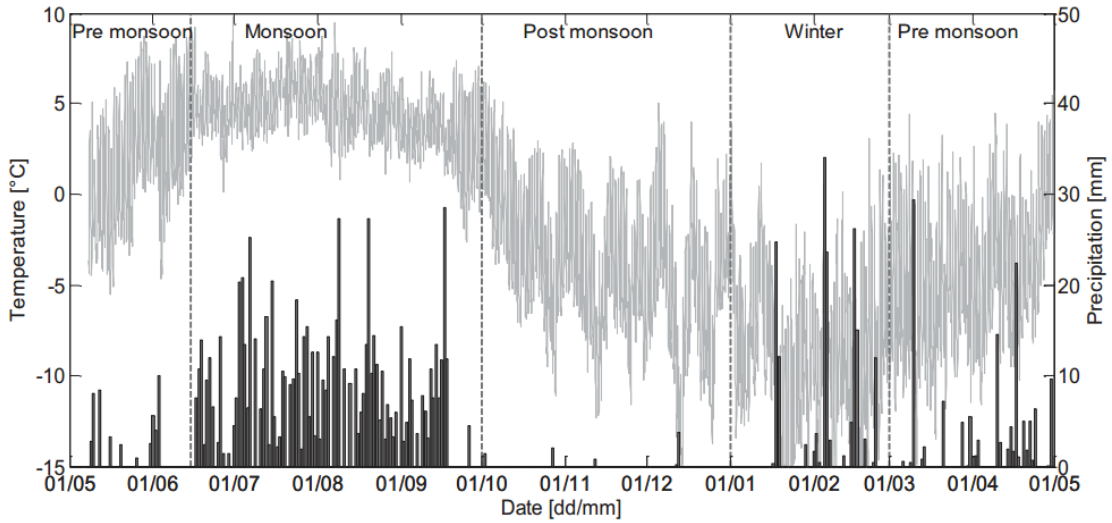

Figure 5. Daily precipitation (bars) and hourly temperature (grey line) at 4831 m station in Langtang Valley between May 2012 and May 2013. Vertical dotted line delineates seasons (from Immerzeel et al., 2014)

The location of the Langtang Valley in the central-eastern Himalaya gives it a monsoon-dominated climate and precipitation regime. Snow accumulation and melt patterns are driven by monsoon-season moisture, temperatures, and cloud cover. The region's glaciers have thus been designated 'summer-accumulation' type (Ageta & Higuchi, 1984). The normal monsoon onset in the region is about 10 June and normal end is about 20 September (DHM). The elevation of maximum precipitation during the monsoon is approximately 2500 m (Figure 6, Baral et al., 2014). The 2008 monsoon onset and retreat occurred on 10 June and 17 October. The 2012 monsoon onset in the Langtang occurred on 17 June, and retreated on the normal day of 20 September. The 2013 monsoon onset date was 14 June and retreat occurred on 19 October.

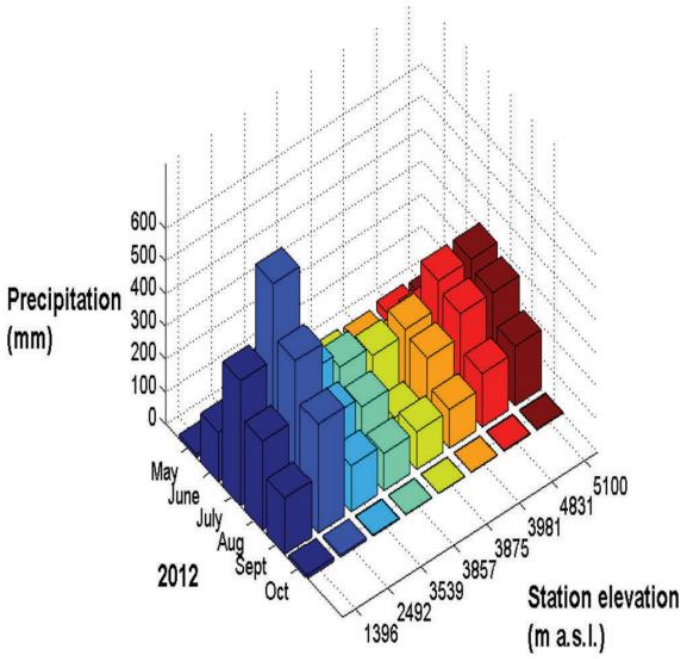

Figure 6. Monthly precipitation in 2012 at different elevations in the Langtang Valley, Nepal (from Baral et al., 2014)

Glacio-hydrological observations in the Langtang Valley have been conducted since 1981 (Higuchi, 1992). Much of the work has focused on mass balance measurements and ground surveys of the Yala Glacier and Lirung Glacier (e.g. Shiraiwa et al., 1992; Yamdata et al., 1992; Kayastha et al., 2003; Yoshimura et al., 2006), but some hydrological and meteorological assessments have also been done (e.g. Fukushima et al., 1987; Takahashi et al., 1987; Motoyama & Yamada, 1989; Seko & Takahashi, 1991; Fujita et al., 1997; Sakai et al., 1997). Shortwave radiation play the dominant role in the heat balance during early summer and late fall, however during the monsoon, the shortwave radiation is reduced when cloud cover is present (Figure 7, Sakai et al., 1998). This has implications for melt rates and associated discharge.

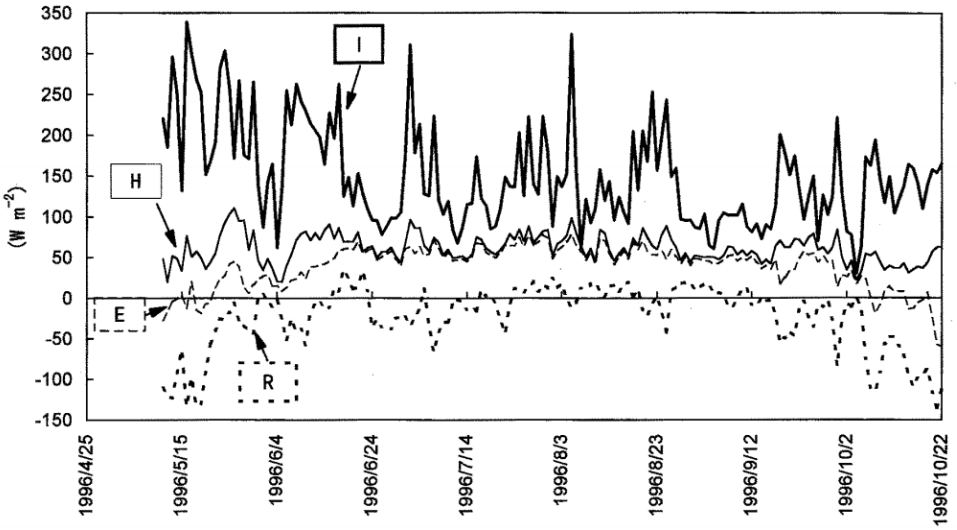

Figure 7. Energy fluxes at an ice cliff surface in the ablation zone of Lirung Glacier from 25 April – 22 October 1996, where I = net shortwave radiation, R = net longwave radiation, H = turbulent sensible heat flux, E = turbulent latent heat flux (from Sakai et al., 1998)

Glacial moraines preserved in the valley floor have been dated with multiple techniques (e.g. carbon and cosmogenic radionuclide) and ages range from 4.98 thousand years old (at elevation 3230 m) to the 20th century (at elevations 3883 m and higher) (Barnard et al., 2006). The presence of unconsolidated glacial landforms down to 3011 m suggests the opportunity for enhanced groundwater retention over a large swath of the basin.

During the May 2012 field campaign, the snow line was observed at approximately 4600 m on the first day (5 May 2012) and fluctuated between 4100 m and 4700 m with precipitation events and subsequent melt. These snow line elevations are above the termini of several glaciers, including Lirung Glacier (~3930m) and the Khimsung Glacier (~4100m).

Weather at Kyangjing during the time period of sampling was recorded to be:

*6 May: Clear skies until afternoon, when it became overcast
*7 May: clear skies until 16:00 when it became overcast, with a cold west wind in the afternoon; snowline estimated at 4700 m;
*8 May: scattered cirrus clouds in morning with a cold wind after 10:00 and cumulus clouds only around the mountain peaks in the afternoon and evening;

*9 May: Overnight precipitation event left a dusting of snow down to 4100 m. Snow line retreated to ~4700 m by mid-afternoon. Clear skies until afternoon when it became overcast
*10 May: Overcast in the morning, with light snow and rain during early afternoon.
*11 May: Clear sky until afternoon when it became partly cloudy
*12 May: Clear sky until afternoon when it became partly cloudy before evening thunderstorms
*13 May: Clear sky until evening when it became partly cloudy.

*19 May: Clear sky until evening when it became partly cloudy.
*20 May: Clear sky until afternoon when scattered clouds formed
*21 May: Clear sky until mid-afternoon when it became overcast
*22 May: Clear sky until mid-afternoon when scattered clouds formed
*23 May: Clear sky until mid-afternoon when scattered clouds formed
*24 May: Clear sky for duration of sampling

3. Methods

3.1 Sample collection

Samples used for analysis were collected during three field campaigns: November 2008 (isotopic values reported in Racoviteanu et al., 2013), the pre-monsoon season of May 2012, and the post-monsoon season of October/November 2013. The May 2012 samples were collected during two separate synoptic surveys and are identified as 'Early May' (6 – 13 May) and 'Late May' (19 – 24 May). Two sets of samples, geochemical and isotopic, were collected during each campaign from surface waters, precipitation, and Langtang River streamwater along an elevational gradient (Table 2). Some sites were only sampled during one season. Sampling locations visited in both seasons include: five Langtang River sites (1479 m to 3745 m); glacier outflow from the Lirung Glacier (4505 m) and the Khimsung Glacier (4166 m); snow samples (4166 m to 5268 m); low-elevation springs inferred to be groundwater (2001 m to 3319 m); a melt stream running parallel to the Lirung Glacier lateral moraine (4134m); Lirung Glacier supraglacial water (4041 m to 4110 m); and a stream originating from an outlet of the clean-ice Yala Glacier (4170 m) sampled 3 km downstream from the terminus in the Lirung sub-basin. Sampling locations visited in only

Table 2. Locations and timing of Langtang River water and its end members, and median values of oxygen-18 isotope data

Site Name	Description	Site code	# pre-monsoon samples	# post-monsoon samples	Elevation	Pre-monsoon $\delta^{18}O$ (‰) (median)	Post-monsoon $\delta^{18}O$ (‰) (median)
Langtang River near Syafrubensi*	River	R1	3	2	1479 m	-13.19	-14.27
Langtang River at Landslide*	River	R2	1	3	1680 m	-13.77	-14.72
Langtang River at Lama Hotel*	River	R3	1	6	2427 m	-14.43	-15.06
Langtang River at DHM gauge	River	R4	2	3	3642 m	-11.83	-15.83
Langtang River at Kyangjing*	River	R5	4	2	3745 m	-12.14	-16.33
Langtang River, Upstream Yala Glacier	River	R6	0	1	3950 m	-12.32	-15.83
Langtang River, downstream Langshisha	River	R7	0	2	4070 m	-12.47	-17.49
Langtang River, upstream Langshisha	River	R8	0	1	4121 m	-12.88	-17.37
Rain	End Member	Rn	2	0	3880 m	-3.80	--
Snow	End Member	sn	3	2	4166 - 5268 m	-7.25	-17.89
Groundwater	End Member	gw	4	10	2001 - 3319 m	-12.29	-13.25
Melt Stream	End Member	Ms	2	3	2459 m	-8.58	-13.66
Khimsung Glacier Outflow	End Member	Km	36	6	4166 m	-13.80	-15.94
Lirung Glacier Outflow	End Member	Li	22	12	3784 m	-10.42	-15.47
Lirung Glacier Ice	End Member	LiI	0	2	4102 – 4235 m	--	-15.93
Lirung Moraine Seepage	End Member	LiM	8	0	3794 – 3796 m	-14.09	--
Lirung Supraglacial	End Member	LiS	5	1	4041 – 4110 m	-11.77	-18.78
Langtang Glacier Outflow	End Member	Lng	0	2	4505 m	--	-17.23
Langtang Glacier Ice	End Member	LngI	0	1	4507 m	--	-16.14
Langshisha Glacier Outflow	End Member	Lsh	0	4	4171 m	--	-17.67
Yala Stream	End Member	YalS	8	2	4170 m	-13.68	-15.75

* = additional November 2008 Langtang River sample

one season included outflow and ice samples from the Langtang Glacier (4505 to 4507 m), outflow from the Langshisha Glacier (4171 m), and outflow seeping from the Lirung terminal moraine (3794 m to 3796 m). Both the Langtang and Langshisha Glaciers have debris-covered tongues.

For a 72-hour window from 6-9 May (Days of Year 127 – 130), an automatic sampler was used to extract Khimsung Glacier outflow every 30 minutes and aggregated four at a time to generate bi-hourly samples. The automatic sampling device was an ISCO 2900 operated with the 24 bottle configuration (500 mL each) and a 7 Ah, 12 V motorcycle battery. The sampling site was 400m downstream of the clean-ice Khimsung Glacier terminus at the location where the stream crosses the terminal moraine (elev. 4166 m). Automatic samplers were emptied at least once every 24 hours to prevent an evaporative signal from the ~3 cm diameter opening on each bottle. Manual samples were collected approximately every three hours during daylight (from 1500 to 2000 hours on 6 May, from 0700 to 2100 hours on 7 & 8 May, and from 0700 to 1300 on 9 May; all times reported in Nepal Time (NPT)) from the Lirung Glacier outflow stream (elev. 3784 m), 400 meters downstream of the debris-covered terminus at a site on the terminal moraine slope. A total of thirty-six Khimsung and twenty-one Lirung samples were collected. These samples allow us to compare the diurnal behavior of debris-covered and clean-ice glaciers.

Sampling protocols (Appendix 1) followed those developed by the Niwot Ridge LTER for high-elevation catchments (Williams et al., 2006). Langtang River water and surface waters were collected as grab samples. Pre-monsoon snow was collected as a 1 m depth-integrated core on the Yala Glacier and post-monsoon snow samples were collected from fresh snowfall and depth integrated over less than 0.5 m. Ice samples were collected from ice faces on the terminus of the Lirung and Langtang Glaciers and intentionally excluded any surface debris. All samples for geochemical analysis were collected in 125 mL HDPE bottles which were soaked overnight with

DI water, rinsed three times with DI water, and rinsed three times with filtered sample water before sample collection. All geochemical samples were filtered in the field within 24 hours of collection using 1.2 µm glass micro-fiber filters. Snow and ice samples were allowed to melt at an ambient temperature and were filtered within 24 hours of melt. Isotopic samples were filtered and stored in 25 mL glass vials with taperseal caps. All samples were stored at ambient temperature until shipment to the University of Colorado Boulder.

Additionally bulk precipitation collectors were installed at four locations along an elevational gradient to characterize the isotopic gradient of monsoon precipitation in the Langtang Valley. Volume was not measured. Bucket locations were: the meteorological stations at Syafrubensi (1460 m) and Kyangjing (3745 m); in a potato field west of Langtang village (~3600 m), next to the house of Cuenga, reader of the DHM water-level gauge on the Langtang River; and at the AWS next to the solar array in the village of Lama Hotel (2430 m). Bulk precipitation collector buckets were constructed and installed following the procedures in Appendix 2, and isotope samples were collected and filtered following the procedures in Appendix 3. Collectors were self-built using supplies that are easily available in Kathmandu. Buckets were installed at the end of May 2012 and were not accessed for sampling until early September 2012. Bulk precipitation results are therefore cumulative for the months of June, July, and August, and are considered to be mean-weighted averages. Bulk precipitation samples were only analyzed for isotopes, since dry deposition of dust and debris into the bucket could influence major chemistry results.

3.2 Laboratory Analysis

Samples from all field campaigns, including 2008, were analyzed for Ca^{2+}, Mg^{2+}, Na^{+}, K^{+}, Cl^{-}, SO_4^{2-}, and oxygen and hydrogen isotopes of the water molecule (^{18}O and deuterium (^{2}H = D)).

Nitrate (NO_3^-) was measured but values were not used in this work due to known non-conservative behavior (Tiemeyer et al., 2008). Samples were analyzed at the Kiowa Wet Chemistry Laboratory run by the NWT LTER at the Institute for Arctic and Alpine Research in Boulder, CO, USA following the protocols presented in Williams et al. (2009). Detection limits for all major solutes were less than 0.2 µeq L^{-1}. Isotopic analysis was conducted using Wavelength-Scanned Cavity Ringdown Spectroscopy (WS-CRDS). All values are reported in micro-equivalents/liter (µeq L^{-1}) except for isotopes, which are reported using the delta (δ) notation as parts per thousand (‰) relative to the Vienna Standard Mean Ocean Water (VSMOW) with a precision of ±0.05‰:

$$\delta^{18}O = \left[\frac{\left(\frac{^{18}O}{^{16}O}\right)_{sample}}{\left(\frac{^{18}O}{^{16}O}\right)_{VSMOW}} - 1\right] \times 1000 \qquad \textit{Equation 1}$$

Deuterium excess was calculated using the equation developed by Johnsen et al. (1989) and has units of parts per thousand (‰):

$$d\text{-}excess = \delta D - 8 * \delta^{18}O \qquad \textit{Equation 2}$$

3.3 Hydrologic mixing models

The objective of hydrologic mixing models is to determine how much water in a river (or other body of mixed water) is generated by each unique source that contributes to stream flow. Mixing models have a range of applications, from estimating underground temperatures in geothermal systems (e.g. Arnórsson, 1985) to extensive applications in remote sensing (e.g. Shimabukura et al., 1991). Hydrochemistry-based hydrologic mixing models mathematically unmix river water based on measured concentrations of one or more chemical tracers in the end member source waters that contribute to discharge. There are five assumptions made about end members and tracers (from Liu, undated):

1. All potential End Members have significantly different concentrations for at least one tracer
2. Tracers are conservative (e.g. no chemical reactions or change of phase)
3. Concentrations of tracers in potential End Members are constant in time or their variability is known
4. Concentrations of tracers in potential End Members are constant in space or they are considered to be from different End Members
5. Unmeasured end members don't contribute significantly to discharge

The first assumption must hold true or the end members are not distinguishable from each other and mathematical solutions for explaining the mixed water will be non-unique. The second assumption is that stream water chemistry is primarily controlled by physical mixing of end members (a linear process) and not by equilibrium chemistry (represented by higher order polynomials) which would be a more complex, and perhaps impossible, accounting task at the basin scale (Christopherson and Hooper, 1992; Hooper, 2003). The second assumption is often not addressed explicitly in mixing models, but can be accounted for by testing whether tracers behave conservatively. The user must reconcile the third and fourth assumptions with the data. In this data set the range of variability is accounted for by using median values in calculations. The fifth assumption is based on how well the chemistry samples represent all potential end members and how well the final mixing model results explain the river water chemistry.

Two-component mixing models can be explored as a first cut at separating melt water from other sources of discharge in glacierized catchments (e.g. Lambs, 2000; Racoviteanu et al., 2013). A two-component mixing model requires a single tracer, as the computational limitation of a sole tracer is differentiating two sources (Figure 8):

$$\mathbf{Q_t = Q_b + Q_r} \qquad \textit{Equation 3}$$

$$\mathbf{Q_t \delta_t = Q_b \delta_b + Q_r \delta_r} \qquad \textit{Equation 4}$$

$$\mathbf{Q_r = Q_t \frac{\delta_t - \delta_b}{\delta_r - \delta_b}} \qquad \textit{Equation 5}$$

Where Q_t is total streamflow discharge (or if calculating percentages it is equal to one), Q_b (e.g. baseflow) is the discharge of the first end member (as a volume or as a percent), Q_r (e.g. rain) is the discharge of the second end member (as a volume or as a percent), δ_t is the concentration of the chosen tracer in the streamflow, δ_b is the concentration of the tracer in the first end member, and δ_r is the concentration of the tracer in the second end member. Because the number of end members is one more than the number of tracers, this avoids an over-determined solution where there are more equations than unknowns.

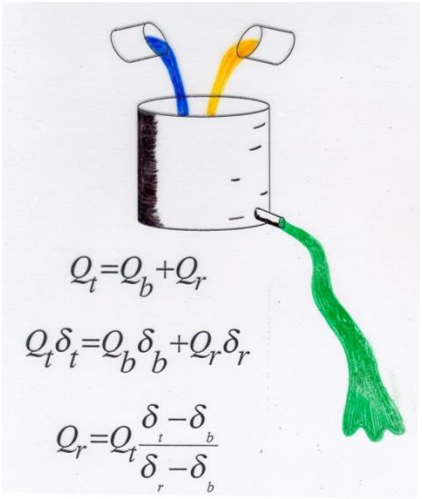

Figure 8. Mixing equations and visualization for two end member mixing model (Vaughn, 1994)

Two component mixing models are limited by their assumption that only two sources contribute to streamflow, which is unlikely to be true all the time in monsoon-influenced, glacierized catchments of the Himalaya where rain, snow melt, glacier melt and groundwater are all likely to contribute significantly to discharge at different times of the year.

3.4 Two-component mixing models

Two-component mixing models using $\delta^{18}O$ as a tracer to unmix Langtang River samples were conducted for the 2012 and 2013 sample sets in order to compare to 2008 results published

by Racoviteanu et al. (2013). The Landslide Hotspring groundwater sample (1680 m) $\delta^{18}O$ values were used for the 2008 and 2012 samples, however the hotspring was inaccessible in 2013 and thus the mean of the 2008 and 2012 samples was used for those samples.

3.5 End Member Mixing Analysis

End Member Mixing Analysis (EMMA) was conducted to determine the source waters that contribute to Langtang River discharge seasonally and along an elevation gradient. EMMA has been developed over the past 25 years (introduced in Christophersen et al., 1990 & Hooper et al., 1990) as multivariate statistical technique for "quantitative representation of the chemical mechanisms that control streamwater chemistry." The original presentation of EMMA was to differentiate soil water end members from different soil horizons, but subsequent hydrological applications have been diverse and often utilitarian – from tracing water pathways in agricultural catchments (Durand & Torres, 1996) to tracking sewage effluent cleanup (Neal et al., 2010).

Christophersen and Hooper's (1992) revision of the EMMA approach introduced the utilization of PCA to reduce the dimensionality of data sets and allow a theoretically indefinite number of measured variables, or tracers (chemical elements, isotopes, and compounds) to inform the mixing model results (Figure 9). By reducing the dimensionality of the data set, the PCA retains most of the information that the tracers contribute. This allows for improved characterization of the uniqueness of each end member. By integrating PCA, EMMA addresses several of the limitations of other hydrologic mixing models, including the pre-selection of end members and over-determination of the mixing equations. Pre-selection of end members is not necessary because EMMA allows for the consideration of as many end members as the user has chemistry data for. Additionally, the PCA reduces the dimensionality of the over-determined streamwater data set, such that the number of principal components retained for use in the final

mixing model is one fewer than the number of end members in the model, thereby avoiding an over-determined solution.

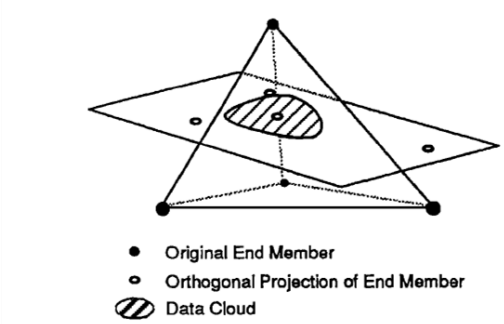

Figure 9. Four end members with two-dimensional mixing space determined by PCA; where the black dots (original End Member) have been re-projected into the 2D plane (white rectangle) and 3 of them will be chosen as the end member contributors to the composition of samples in the striped data cloud (from Christophersen and Hooper, 1992)

The amount of information retained by the principal components, which are eigenvectors of the streamwater data matrix, is assessed with the proportion of variance values derived from the eigenvalues of the data matrix. Proportion of variance is the amount of variability in the data set explained by each principal component, or eigenvector. Proportion of variance allows the user to decide how many principal components to consider in subsequent analysis to unmix the streamwater. When the samples are projected into PCA space, which has reduced dimensions defined by the streamwater's principal components, the presence of high residuals between original tracer values and projected values indicates that the tracer is not well explained by the principal components and could be a sign that the tracer in question exhibits different, possibly non-conservative, behavior in the system (Hooper, 2003).

When utilizing PCA, the basic steps in the EMMA process are:

1. Compile streamwater and end member data, including all available end member samples but only including tracers for which all samples have measured values
2. Determine, subjectively, which tracers in the streamwater data set are conservative

3. Run PCA on the streamwater samples using only the conservative tracers, and examine proportion of variance explained by each component
4. Choose, somewhat subjectively, how many components to retain from the PCA based on eigenvalues or proportion of variance explained by each component
5. Project all of the samples into the space defined by the retained PCA components using the conservative tracers from both streamwater and end member samples
6. Choose a number of end members (equal to the dimension of the PCA space plus one) which will be used to explain the streamwater chemistry – the chosen end members should circumscribe the streamwater data cloud,
7. Based on Euclidean distance calculate the proportion that each end member contributes to the composition of a streamwater sample.

Sampling strategy for EMMA work must include water from all potential end members as well as the river water that is being unmixed. The same chemical species, or tracers, should be measured for each sample to create the EMMA data set (step 1). All of the tracers used as input for the PCA must first be defined as conservative (step 2). The PCA (step 3) is run on the mixed streamwater samples and does not include end member chemistry data. Once conservative tracers are chosen and the PCA is conducted, the user has a subjective choice of how many principal components to retain in order to best define the mixed water (step 4). Eigenvectors produced by the PCA (step 4) form the basis for a new Euclidean space into which both streamwater and end members are projected (step 5). The method used here is the 'Rule of One', which states that only the PCA's eigenvectors with eigenvalues which explain more than any one of the single original variables, i.e. with a value greater than one, should be retained. Another approach is setting a threshold of proportion of variance explained. Fengjing Liu has produced an EMMA tutorial (Liu, undated) which advises retaining as many components as necessary to have 90% (or a different user-defined threshold value) of the variance explained. Eigenvectors of the principal components that are retained define a dimension of the reduced-dimensionality subspace in which all of the data will be projected and from which contributing end members chosen (Christophersen & Hooper, 1992). Multiple end members can be plotted, but end members chosen to explain the

streamwater chemistry composition must number one greater than the subspace dimension (step 6). Chosen end members will circumscribe the projected mixed streamwater samples (Figure 9) and contributions to each streamwater sample are determined based on Euclidean distance (step 7). In this data set, projection of the chemistry data into space defined by two principal components produced a three-component EMMA.

The final calculation of percent contribution uses:

$$1\mathbf{a_1} + \mathbf{a_2} + \mathbf{a_3} \qquad \textit{Equation 6}$$

$$\mathbf{SW_{U1}} = \mathbf{a_1 EM_{1U1}} + \mathbf{a_2 EM_{2U1}} + \mathbf{a_3 EM_{3U1}} \qquad \textit{Equation 7}$$

$$\mathbf{SW_{U2}} = \mathbf{a_1 EM_{1U2}} + \mathbf{a_2 EM_{2U2}} + \mathbf{a_3 EM_{3U2}} \qquad \textit{Equation 8}$$

where a_1, a_2, and a_3 are the fractions of each end member, SW_{U1} and SW_{U2} are the projected streamwater values in Euclidean space coordinates, and EM_{nU1} and EM_{nU2} are the coefficients of the nth end member projected in PCA space (Barthold et al., 2011, modified from Christopherson et al., 1990; and Liu et al., 2004).

Hooper et al. (2003) suggested an improvement on the previous approaches for choosing conservative tracers, noting that streamwater tracer values can be projected in the Euclidean space defined by the PCA. Once projected, the residuals (the difference between original tracer concentration values and the values when the tracer is projected into the mixing space) can be examined for structure. Structure in the residuals indicates that the data does not fit well in the Euclidean space and that an additional dimension should be added so that more of the data is explained and the residuals become random. While mathematically more robust, this approach introduces subjectivity as the user defines whether residuals have structure or not. It also requires a sample size large enough to offer confidence in the statistical significance, or lack thereof, of a linear trend.

Geochemical and isotopic tracers were determined to be conservative following Hooper (2003), and proportions of flow were assigned to end members using the Principal Component Analysis (PCA) methodology of Christophersen and Hooper (1992).

4. Results and Discussion

4.1 Chemistry and Isotopic Tracers

Precipitation and ice samples exhibit wide variability in isotopic values but concentrations of chemical solutes were consistently low with the exception of sodium and chloride (Figure 10). Ice samples (n=3) generally had solute concentrations less than than 5 μeq L^{-1}, with maximum concentrations (e.g. sodium, 24 μeq L^{-1}) always less than 25 μeq L^{-1}. Pre-monsoon rain (n=2) had elevated sodium (107 μeq L^{-1}) and chloride (47 μeq L^{-1}) concentrations, about five times that of mean values for glacier ice and snow. Marine air masses, such as those that bring monsoonal moisture, can also have elevated sodium and chloride (Junge & Werby, 1958), and this likely influences the 11 May 2012 rain samples. Both pre-monsoon snow (n=3) and post-monsoon snow (n=2) had sodium and chloride concentrations less than 25 μeq L^{-1}, but post-monsoon snow had a maximum calcium value (68 μeq L^{-1}) nearly double the maximum in pre-monsoon snow (40 μeq L^{-1}). Concentrations of calcium, sodium, and chloride in the pre-monsoon snow samples are comparable to values found in snow from the northern and western Tibetan Plateau and attributed there to dust sources (Wake et al., 1993; Thompson et al., 2000). Solute concentrations in both pre- and post-monsoon snow samples are up to an order of magnitude higher than those reported for rain in the Khumbu Valley (Marinoni et al., 2001), though spatial and temporal variability in precipitation solute concentrations, particularly in snow, is not well-constrained in the region.

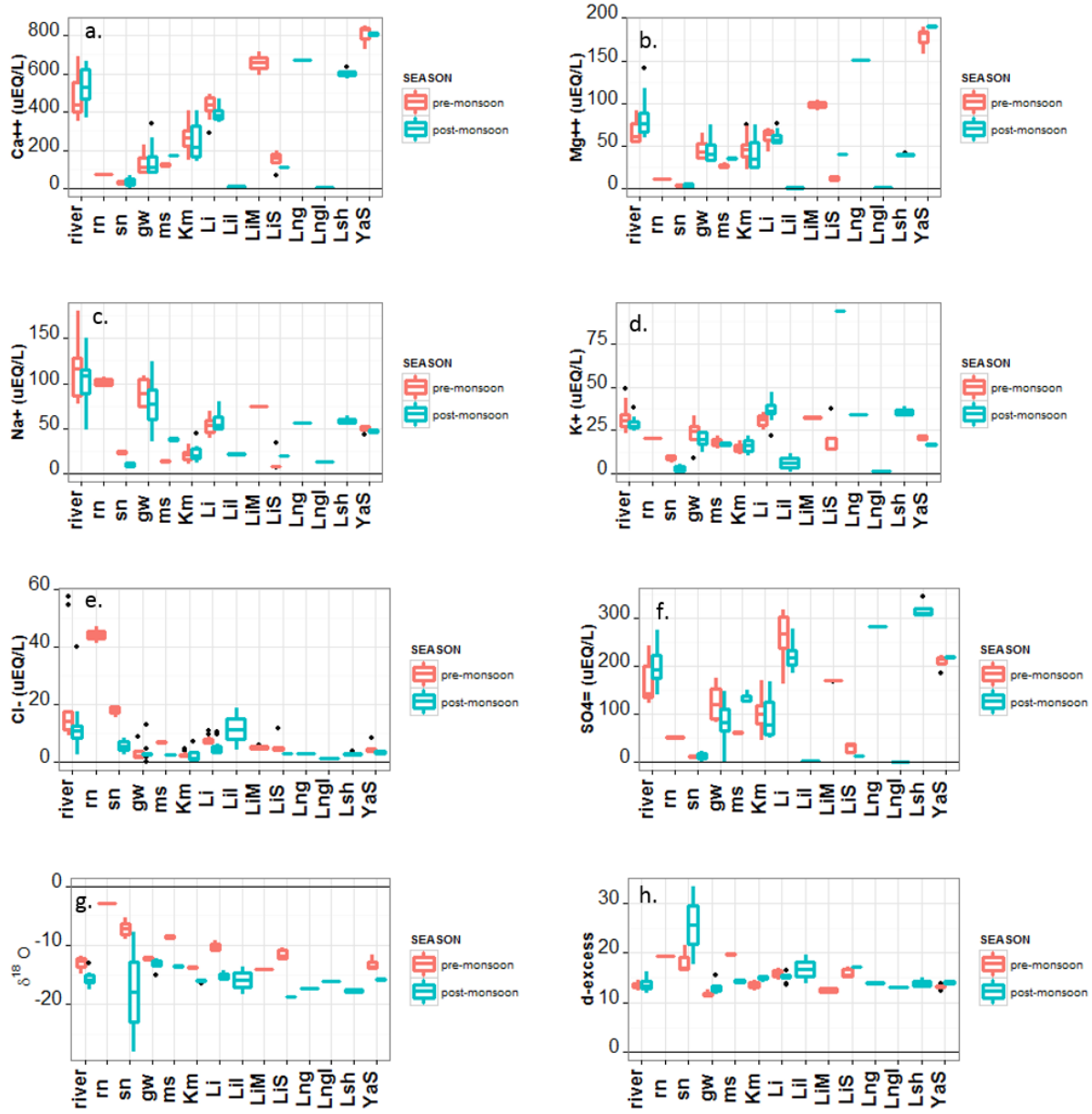

Figure 10. Boxplots comparing pre-monsoon (May 2012) and post-monsoon (October/November 2013) values of geochemical and isotopic tracers in Langtang river water and its end members: rain (rn), snow (sn), groundwater (gw), melt stream (ms), Khimsung Glacier (Km), Lirung Glacier (Li), Lirung Glacier Ice (LiI), Lirung Moraine (LiM), Lirung Supraglacial (LiS), Langtang Glacier (Lng), Langtang Glacier Ice (LngI), Langshisha Glacier (Lsh), Yala Stream (YaS)

Outflow from the Khimsung, Lirung, Langtang, and Langshisha Glaciers had solute concentrations that exceed those of snow or rain generally by an order of magnitude, with the exceptions of sodium and chloride, which were highest in rain (Figure 10). Geochemical tracer concentrations were generally higher in the debris-covered Lirung, Langtang, and Langshisha Glaciers relative to the clean-ice Khimsung Glacier. For the two glaciers where we have pre- and post-monsoon samples, the Lirung and Khimsung Glacier outflow, geochemical tracer concentrations were in the same range, suggesting little seasonal change in solute concentrations in the non-monsoon season.

Lirung moraine seepage, Langtang Glacier outflow, Langshisha Glacier outflow, and the Yala Stream all had calcium concentrations above 600 μeq L^{-1}. Magnesium concentrations were highest in Langtang Glacier outflow (150 to 151 μeq L^{-1}), and the Yala Stream (pre-monsoon: 158 to 190 μeq L^{-1} and post-monsoon 189 to 191 μeq L^{-1}). These same sites, along with Lirung Glacier outflow, and post-monsoon Langtang River water, had the highest concentrations of sulfate (>170 μeq L^{-1}). Elevated values of calcium, magnesium, and sulfate are attributed to post-precipitation processes and they help define reacted versus unreacted waters.

Examining May 2012 pre-monsoon and November 2013 post-monsoon isotope results , Langtang River water samples have δD versus $\delta^{18}O$ values that plot along the Global Meteoric Water Line (GMWL = 8x + 10) [Craig, 1961] (Figure 11). The GMWL is the worldwide average of hydrogen and oxygen isotope ratios in terrestrial waters, and waters that plot along the line generally have not undergone evaporative processes (Dansgaard, 1964). All Langtang River $\delta^{18}O$ values fall within the range of -11‰ to -17‰ (Figure 11). The May 2012 Langtang River samples have a $\delta^{18}O$ range of -11.8‰ (Site R1, 20 May) to –14.8‰ (Site R5, 8 May). The δD versus $\delta^{18}O$ relationship for the pre-monsoon river samples has a slope of 8.4 (R^2 = 1.00), compared to the

GMWL slope of 8.0. The post-monsoon October/November 2013 Langtang River samples have a $\delta^{18}O$ range of -14.8‰ (Site R2, 12 Nov) to –17.5‰ (Site R7, 21 October). Their δD versus $\delta^{18}O$ slope was 7.5 (R^2 = 0.99). In November 2008, the slope was 6.7 (R^2 = 1.00). The most enriched $\delta^{18}O$ value (-12.8‰) was at site R1 and the most depleted (-15.2‰) was at site R7. The decrease in slopes in both post-monsoon data sets indicates kinetic fractionation may have affected the isotope ratios.

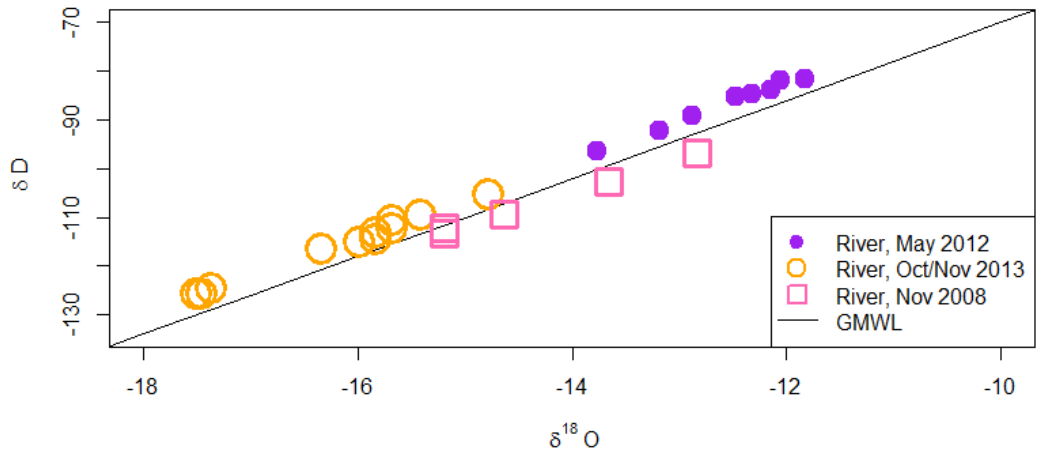

Figure 11. Langtang River water samples relative to the Global Meteoric Water Line

Apart from Langtang River water, there was a large range in the isotopic values of both precipitation and surface waters (Figure 10g). The $\delta^{18}O$ values in precipitation ranged from a post-monsoon snow value of -28.1‰ to the most enriched value in pre-monsoon rain (11 May) at Kyangjing of -2.8‰. It is noteworthy that the post-monsoon snow samples have a wide range of $\delta^{18}O$ values (-28.1‰ to -7.7‰). Lirung Glacier outflow, melt stream samples, and supraglacial water had the largest range in between the pre- and post-monsoon, with median values decreasing by -4.8‰, -5.1‰, and -7.0‰, respectively. Khimsung Glacier outflow median values decreased by 2.1‰. The smallest magnitude of change in $\delta^{18}O$ between the seasons was in the low-elevation

groundwater samples (-1.0‰), suggesting they are well-integrated over time. The depletion of $\delta^{18}O$ values in the post-monsoon relative to the pre-monsoon in river water, precipitation and glacier outflow is generally associated with source moisture of cooler temperatures, possibly late monsoon precipitation. Values of $\delta^{18}O$ are known to be enriched during the monsoon relative to other times of year, in Kyangjing peaking at around -5 ‰ in early summer and becoming depleted to around -20 ‰ by early winter (Zhang et al., 2001).

The similarity between pre-monsoon and post-monsoon geochemistry for outflow at both the Lirung and Khimsung Glaciers, despite differences in $\delta^{18}O$ values, signifies that precipitation arriving in different seasons follows similar flow paths over a comparable time frame, and thereby acquires similar solute concentrations. Future collection of monsoon-season samples of glacier terminus outflow would offer insight into this behavior.

Isotopic results from the monsoon bulk precipitation samples along an elevational transect (Figure 12), which are an aggregate of June-August rain in the Langtang Valley, yield a Local Meteoric Water Line (LMWL) of:

$$\mathbf{LMWL_{precipitation} = 7.94x + 9.2} \qquad \textit{Equation 9}$$

$$(r^2 = 1.000, p - value < 0.05)$$

The monsoon precipitation $\delta^{18}O$ values ranged from -9.7‰ at Syafrubensi to -14.9‰ at Kyangjing with a monsoon mean of -12.94‰. The lapse rate, change in $\delta^{18}O$ per meter of elevation gain, is calculated using the bulk precipitation samples collected from the four elevations over the duration of the 2012 summer monsoon:

$$\mathbf{y = -0.0023x - 6.26} \qquad \textit{Equation 10}$$

$$(r^2 = 0.989,\ p - value < 0.01)$$

Which yields a change of 2.3 ‰ depletion per kilometer of elevation gain. This is on par with the global average relationship between precipitation and elevation of 2 ‰ depletion per kilometer of elevation gain (Bowen & Wilkinson, 2002).

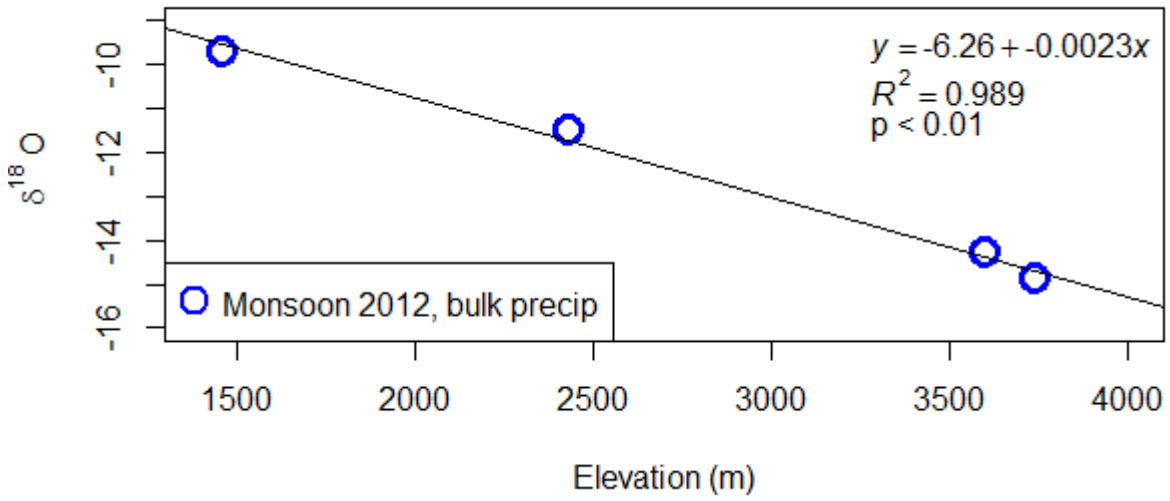

Figure 12. Isotopic gradient of 2012 monsoon precipitation in the Langtang Valley

Variability in $\delta^{18}O$ values in precipitation in the Langtang Valley has been studied before. Zhang et al. (2001) published a study of precipitation samples collected daily at Kyangjing (3380m) from May 1993 to October 1996, and of values in precipitation collected at stations in Kyangjing and at Yala Glacier base camp (5100m) in 1996. Isotope results from daily samples were weighted by precipitation volume in order to present a weighted mean $\delta^{18}O$ value for each month. Using values estimated from Zhang et al.'s (2001) published data (Figure 13) to generate an aggregated 3-month $\delta^{18}O$ value, the Kyangjing cumulative weighted mean $\delta^{18}O$ value for June, July, and August precipitation are calculated to be approximately -13.4‰ in 1993, -16.3‰ in 1994, -17.3‰ in 1995, and -16.0 in 1996. While the 3-month summer aggregated value we measured at Kyangjing in 2012 of -14.9‰ is within the range of values found in the mid-1990s, the Zhang et al. (2001) data shows the high interannual variability of oxygen isotope values in precipitation at

Kyangjing during the monsoon. They also found a weak but statistically significant negative correlation between amount of precipitation and $\delta^{18}O$ value. Precipitation volume in 2012 was not readily available, so this correlation was not tested.

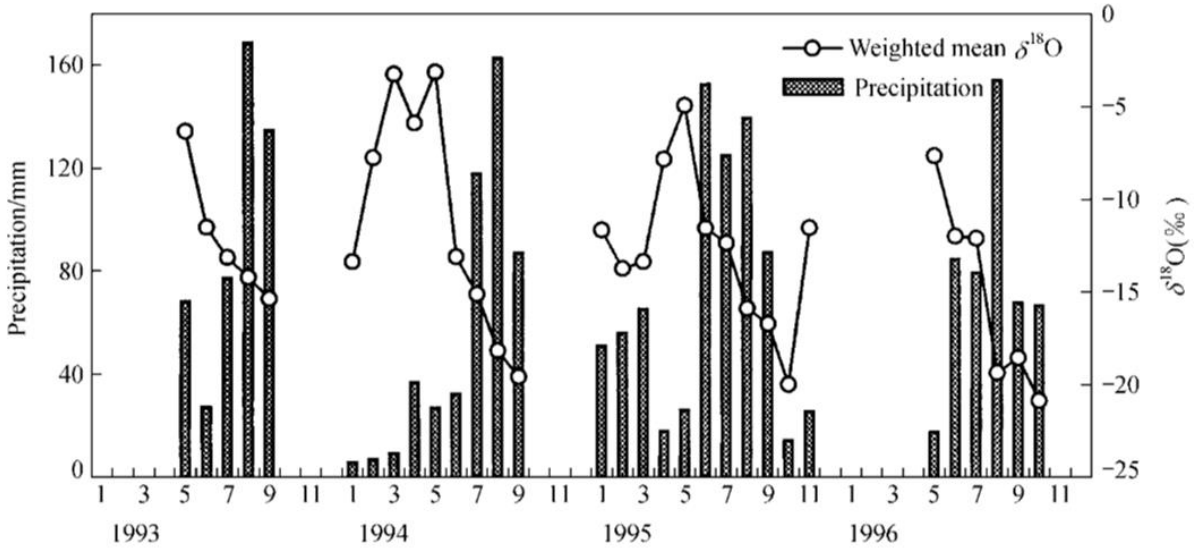

Figure 13. Monthly variations of the weighted mean δ18O and precipitation at Kyangjing from May, 1993 to October, 1996. (Zhang, 2001)

Establishing a correlation between elevation and $\delta^{18}O$ values in Langtang River Basin precipitation is an important step for future hydrological modeling in the basin. Blasch & Bryson (2007) showed that regardless of interannual variability of isotope values, the trend itself remains nearly constant over time and between seasons. While additional sampling is required to verify the assumption that Equation 10 holds over time in the Langtang River Basin, it presents the opportunity of minimizing future field efforts by sampling precipitation at a single site and extrapolating to other elevations using the known gradient.

4.2 Diurnal behavior of clean-ice and debris-covered glaciers

Bihourly samples collected over a 72 hour window in May 2012 show distinct differences between the geochemistry and isotopic content of outflow from the clean-ice Khimsung Glacier and the debris-covered Lirung Glacier. Khimsung isotopic tracers had a range of $\delta^{18}O$ values from

-14.1‰ to -13.6‰ with a median of -13.8‰, and a d-excess range of 12.4‰ to 14.4‰ with a median of 13.5‰ (Figure 14). In contrast, the $\delta^{18}O$ values in Lirung glacier outflow were relatively enriched, ranging from -11.2‰ to -9.3‰ and with a median of -10.4‰, and d-excess values ranging from 14.6‰ to 17.1‰ with a median of 15.6‰. Values of $\delta^{18}O$ and d-excess were statistically different between the two glaciers' outflow based on an unpaired Mann-Whitney test ($p << 0.01$, $n_{Km} = 36$, $n_{Li} = 22$). For both sites, there was as well a temporal change in the isotopic content. In the Khimsung outflow, the increase in $\delta^{18}O$ values was small but statistically significant (slope = 0.08 ‰ d^{-1}, $R^2 = 0.171$, $p = 0.04$). In the Lirung outflow during the sampling period, the increasing trend in $\delta^{18}O$ was an order of magnitude greater (slope = 0.7 ‰ d^{-1}, $R^2 = 0.908$, $p<<0.01$). Deuterium-excess values behaved similarly: at Khimsung there was a low slope that was not statistically significant, and at Lirung there was a significant increase of 0.6 ‰ d^{-1} ($R^2=0.566$, $p<<0.01$). For both $\delta^{18}O$ and d-excess, Lirung Glacier outflow values were more enriched than Khimsung Glacier outflow values. Additionally there was a strong enrichment over time for Lirung outflow and a more muted change in Khimsung outflow for these two parameters

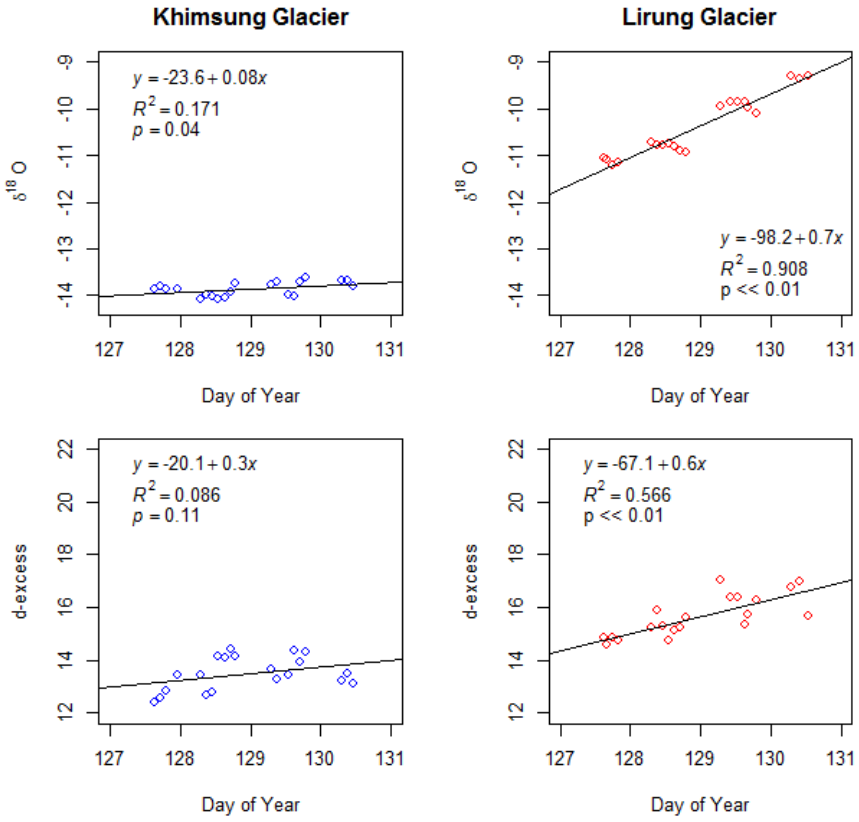

Figure 14. Isotopic trends for bihourly sampling at the clean-ice Khimsung Glacier and the debris-covered Lirung Glacier in May 2012

The increasing trend of $\delta^{18}O$ and deuterium-excess values in the debris-covered Lirung Glacier relative to the clean ice Khimsung Glacier could be attributable to more melt/freeze episodes for the debris-covered glacier compared to the debris-free glacier. Contact between liquid water and frozen water will preferentially remove lighter isotopes from the ice of a glacier, enriching the isotopic signal of the remaining ice (Taylor et al. 2002; Williams et al. 2006). The presence of debris, which alters albedo and insolation dynamics, is known to facilitate a higher number of melt/freeze cycles, which in turn can elevate d-excess and enrich the remaining ice 2‰ to 3‰ in $\delta^{18}O$ (Steig et al., 1998), similar to the difference we see in outflow samples from the Lirung and Khimsung Glaciers. Isotopic fractionation may also play a role, as the first melt water to leave seasonal snowpack is the most depleted (Williams et al., 2009). Changes in $\delta^{18}O$ and d-

excess values of the Khimsung Glacier are small over the three day window, suggesting melt-freeze cycles and isotopic fractionation of snowpack do not play a strong role in the isotopic history of the clean-ice glacier outflow.

Geochemical tracer concentrations for the debris-covered Lirung Glacier outflow were consistently higher and had less amplitude in their variation than the debris-free Khimsung Glacier outflow (Figure 15). Calcium concentrations in Lirung outflow ranged from to 358 to 493 μeq L^{-1}, with an amplitude as small as 30 μeq L^{-1} d^{-1}. In Khimsung outflow the range of calcium values was 147 to 409 μeq L^{-1} with a daily amplitude of at least 100 μeq L^{-1}. Similarly, for the Lirung outflow concentrations of sulfate ranged from 200 to 317 μeq L^{-1}, while Khimsung outflow ranged from 47 to 169 μeq L^{-1}. Thus, minimum concentrations of sulfate from the Lirung glacier were greater than maximum concentrations of sulfate from the Khimsung glacier. Elevated calcium and sulfate concentrations are consistent with debris influencing the solute loads of the glacier outflow. In contrast, chloride concentrations were much lower than the geochemical weathering products, ranging from 6.4 to 9.6 μeq L^{-1} in the outflow of the Lirung glacier and1.6 to 4.7 μeq L^{-1} from the Khimsung. These low values of chloride are consistent with the low values in snow and ice and much lower than in rain, suggesting that monsoon rain at these elevations and in these seasons makes little contribution to glacier discharge.

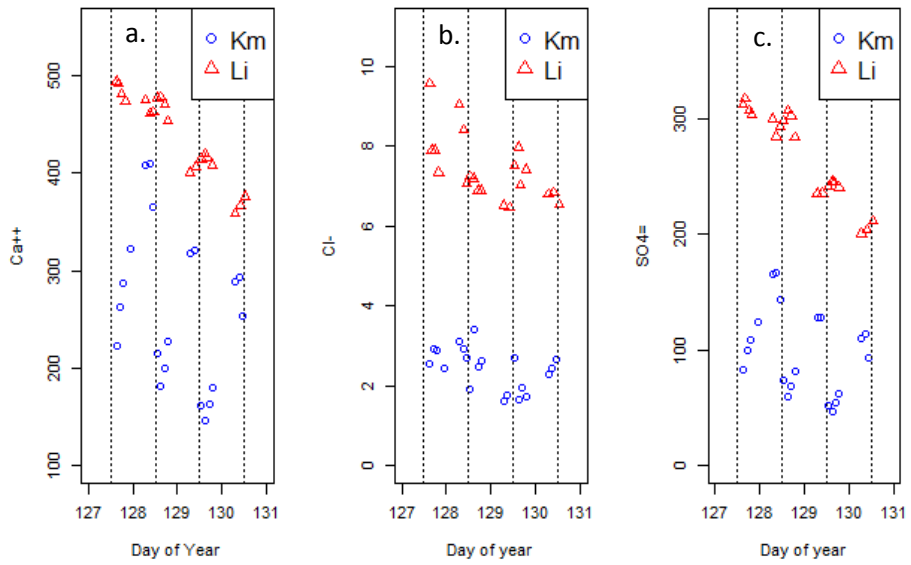

Figure 15. Select geochemical tracer trends for bihourly sampling at the clean-ice Khimsung Glacier and the debris-covered Lirung Glacier in May 2012. Vertical dashed lines mark noon for each day

Diurnal trends in geochemical tracer concentrations were more pronounced in Khimsung Glacier outflow relative to Lirung Glacier outflow. With the exception of chloride, Khimsung Glacier outflow peaked in solute concentration for all geochemical tracers each morning in samples collected either at 0700 or 0900. Minimum daily concentrations for those tracers occurred in either the 1300 hour or 1500 hour. This pattern of decreasing geochemical weathering products during the daytime may be attributable to dilution by clean snow and ice melt when peak melting occurs in the middle of the day (Williams et al., 2006). Snow and ice melt declined in the later hours of the afternoon and may have stopped completely in the night. While englacial or subglacial storage can create a lag between discharge maxima and solute concentration minima (Anderson, et al., 2003) the correlation at Khimsung Glacier between dilution of solute concentrations and time of maximum melt suggests there is very little lag and that daily snow/ice melt dilution drives

the chemograph patterns. Diurnal trends in solute concentrations for Lirung outflow, in contrast, were of smaller magnitude, suggesting larger sub-glacial storage and less clean snow/ice melt.

4.3 Langtang River hydrograph Separation

4.3.1 Mixing models

Following the approach of Racoviteanu et al. (2013), two-component mixing models using $\delta^{18}O$ as the sole tracer were conducted for the 2012 and 2013 Langtang River water samples (Table 3). Groundwater for all versions of the mixing model was parameterized using the $\delta^{18}O$ value of water at the Landslide hotspring (1680 m). In 2008 Racoviteanu et al. (2013) measured an $\delta^{18}O$ value of -13.3‰, and in May 2012 we measured -13.6‰. The hotspring was inaccessible in 2013 and thus the mean value of the 2008 and 2012 samples was used to represent groundwater (-13.5‰). Melt water for the 2008 mixing model was parameterized by Racoviteanu et al. (2013) using outflow from the Langtang Glacier (-15.5‰). For 2012, melt water was represented by the mean of the high-frequency Khimsung Glacier outflow samples (-13.8‰). For 2013 samples, outflow from the Langtang Glacier (-17.3‰) was used to represent melt water.

Table 3. Two-component mixing model results for three years of Langtang River water samples

Site	Date	Ground water	Melt water	Rain/snow
R1*	23 Nov 2008	73%	27%	--
R3*	24 Nov 2008	63%	37%	--
R4*	25 Nov 2008	30%	70%	--
R1	20 May 2012	355%	-255%	--
R2	20 May 2012	316%	-216%	--
R3	21 May 2012	293%	-193%	--
R4	22 May 2012	275%	-175%	--
R5	22 May 2012	221%	-121%	--
R1	20 May 2012	--	30%	70%
R2	20 May 2012	--	73%	27%
R3	21 May 2012	--	75%	25%
R4	22 May 2012	--	77%	23%
R5	22 May 2012	--	81%	19%
R1	19 Oct 2013	52%	48%	--
R2	19 Oct 2013	41%	59%	--
R3	20 Oct 2013	37%	63%	--
R4	21 Oct 2013	24%	76%	--

For the November 2008 samples at the R1, R3, and R4 sampling sites, Racoviteanu et al. (2013) estimate 27%, 37%, and 70% melt water contributions using $\delta^{18}O$ as the sole tracer. The rest was assumed to be groundwater. Langtang River samples from the Late May 2012 synoptic survey had $\delta^{18}O$ values more enriched than either the Landslide hotspring groundwater or the Khimsung Glacier outflow, resulting in non-plausible results in which all estimates are outside the range of 0% to 100% (Liu et al., 2004). Given that the Late May samples were collected during snow and ice melt, an alternative two-component mixing model using the median of May 2012 rain and snow samples (-5.3‰) was run. These results are all within the realistic range of 0% to 100%, with estimates of 81% meltwater at R5 and declining to 30% at R1. Post-monsoon estimates in 2013 were 76% melt water at R4, declining to 48% melt water at R1.

October 2013 melt water estimates are higher than estimates for the same sites in November 2008, potentially attributable to November 2008 $\delta^{18}O$ values being closer to those of baseflow versus seasonal melt values. The May 2012 $\delta^{18}O$ values are more enriched than groundwater but less enriched than new precipitation suggest that during that synoptic survey rain and snow melt contribute significantly to river discharge. This introduces some skepticism about the ability of two-component mixing models using $\delta^{18}O$ values to confidently unmix river water, particularly given the possibility that more than two sources contribute significantly to discharge at any given time in the Langtang River basin. Conducting a three-component EMMA allowed us to explore this further.

4.3.2 End Member Mixing Analysis (EMMA)

Langtang River water samples from four synoptic surveys in three different years show consistent enrichment in $\delta^{18}O$ values with decreasing elevation and a simultaneous decrease in geochemical weathering products (Figure 16). These spatial patterns suggest that reacted waters

are primarily generated from debris-covered glaciers and moraine seepage in the Upper Langtang Basin and they become diluted at lower elevations. The late May synoptic survey stands out as having the lowest concentrations of calcium, magnesium, sodium and sulfate, and the most enriched $\delta^{18}O$ values. The pre-monsoon rain and snow had the most enriched $\delta^{18}O$ values in precipitation. The large amount of chemistry dilution and enrichment of water isotopes from the early May 2012 samples to late May 2012 suggests that new snow melt and rain entered the hydrologic system at this time. In contrast, sodium and chloride concentrations showed lower variability with elevation. Most likely this is because these solutes are largely sourced from precipitation and not affected by the geochemical weathering that generates reacted waters.

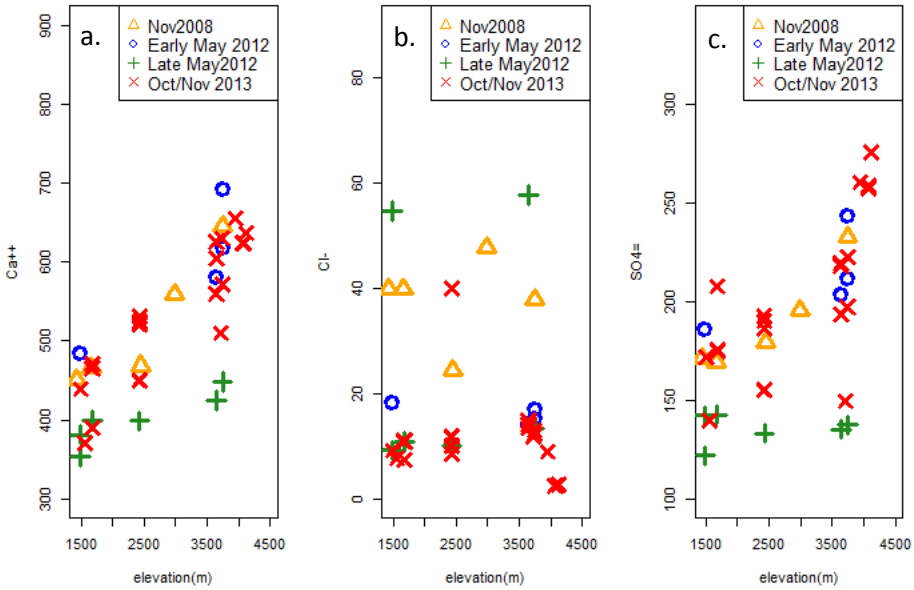

Figure 16. Trends in Langtang River water chemistry by season

To improve our understanding of source waters and flowpaths to the Langtang River we applied EMMA to all river samples collected over the four expeditions. We then plotted potential end-members (using the median when there was more than one sample) into the PCA space

generated by the chemistry of the tracers in river water. Application of EMMA indicated that seven tracers were deemed conservative using the Hooper (2003) method (calcium, magnesium, sodium, potassium, chloride, sulfate, and $\delta^{18}O$). PCA analysis (Table 4) found two eigenvalues greater than one (as required by the Rule of One), suggesting three end-members contributed the majority of water to the Langtang River (Figure 6). Together these two eigenvectors explained 84% of the variance in chemistry tracer data, shy of the 90% preferred meaning there may be another unmeasured end-member.

Table 4. Principal Component Analysis results for the Langtang River samples using seven tracers.

	PC1	PC2	PC3	PC4	PC5	PC6	PC7
Eigenvalue	1.9409	1.4622	0.77194	0.52888	0.33040	0.27603	0.18351
Proportion of Variance	0.5382	0.3054	0.08513	0.03996	0.01559	0.01088	0.00481
Cumulative Proportion	0.5382	**0.8436**	0.92875	0.96871	0.98430	0.99519	1.00000

Not all of the end members that were sampled were unique. When the seven geochemical and isotopic tracer values were considered in the EMMA, the end member samples clustered in two main groups (Figure 17). At the upper left of the EMMA plot, the unreacted meltwater cluster includes ice samples from the Lirung and Langtang Glaciers, outflow at the terminus of the Khimsung Glacier, and both pre- and post-monsoon samples from the meltwater stream. As the original source of all water in the catchment, the snow samples and pre-monsoon rain plot on the periphery of the unreacted meltwaters. The reacted cluster on the right side of the plot includes outflow from the three debris-covered glaciers (Langtang, Lirung, and Langshisha), the down-valley Yala Stream and Lirung moraine seepage. Lirung supraglacial water plots with the unreacted samples in the pre-monsoon, and alone in the lower left in the post-monsoon. Neither

Lirung nor Khimsung Glacier outflow samples vary in their PCA characterization between the pre-monsoon and the post-monsoon.

The points chosen to best bound the data cloud of river water samples were: Langtang Glacier outflow, Khimsung Glacier outflow, and a Langtang River water sample from Late May 2012 collected at the DHM gaging station (site R4 in Figure 1). The river water sample was used as a proxy to represent a monsoon-influenced end member that we hypothesize our data set is missing. The lower-left samples were interpreted as monsoon-influenced based on elevated sodium and chloride values, associated with marine-sourced precipitation (Junge & Werby, 1958), and enriched $\delta^{18}O$ values also associated with the early monsoon (Zhang et al., 2001). The river sample chosen as the proxy end member had a sodium concentration 20% higher than the median for river samples (129 μeq L^{-1} vs 110 μeq L^{-1}), and a chloride concentration four times higher than the river sample median (49 μeq L^{-1} vs 12 μeq L^{-1}). The $\delta^{18}O$ value was -12.47‰ compared to the river sample median of -14.99‰. The monsoon-influenced end member proxy had calcium, magnesium, potassium, and sulfate concentrations comparable to Lirung Glacier outflow, implying the water has been routed through the subsurface and acquired a reacted solute profile.

In the EMMA analysis, the six Late May samples plot to the left of the other synoptic surveys and furthest from the reacted water end member (Figure 17). The November 2008 samples also cluster away from the reacted end member. Four of the October/November 2013 samples which are closest to the Langtang Glacier end member (sites R6, R7, R8, and R9) were all collected at elevations above 3745 m, the maximum elevation of other surveys. The chosen end members were used to calculate composition of river water, which yields percent estimates of reacted meltwater, unreacted meltwater, and monsoon-influenced water in the river (Table 5). River

samples plotting outside the bounding triangle were moved to the line using the methodology of Liu et al. (2004).

At the lowest elevation site, R1, reacted meltwater contributed more than 20% of discharge in Early May and Oct/Nov, and more than 15% in November 2008. These are the seasons closest to base flow. During Late May, estimates of reacted meltwater contribution declined to 0% and 6% for the two available samples with unreacted meltwater and monsoon-influenced water becoming dominant. At the highest site sampled in all four surveys, R5, reacted meltwater dominated in the early May samples (59% on 8 May and 46% on 10 May), but unreacted meltwater played a large role in Late May (45%). The early May and late May synoptic surveys were less than three weeks apart but show a strong shift towards snow melt and rain influence.

In May 2012, DHM recorded 14.8 mm of precipitation at Kyangjing and this may have been sufficient to initiate groundwater movement in a piston-style influx to the river (Buttle, 1994), especially in the Upper Langtang Basin. Field observations of an increase in discharge volume and the presence of groundwater springs below 3000 m, which is the inflection from U-shaped glaciated valley above to non-glaciated terrain below, are attributable to the decrease in groundwater storage capacity in the bedrock below the inflection as compared to the

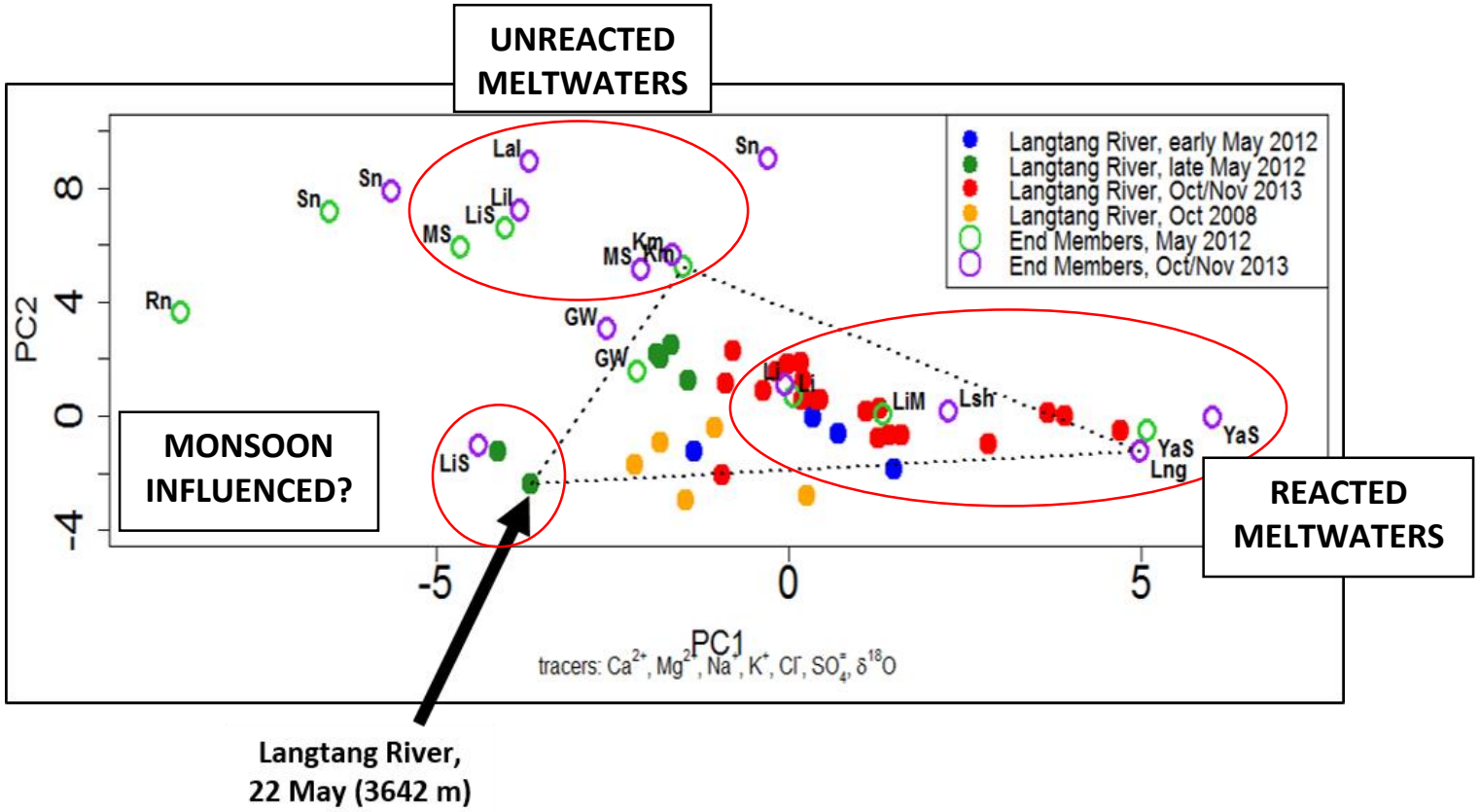

Figure 17. EMMA results for three seasons of Langtang Valley water samples. Where: rain (rn), snow (sn), groundwater (gw), melt stream (ms), Khimsung Glacier (Km), Lirung Glacier (Li), Lirung Glacier Ice (LiI), Lirung Moraine (LiM), Lirung Supraglacial (LiS), Langtang Glacier (Lng), Langtang Glacier Ice (LngI), Langshisha Glacier (Lsh), Yala Stream (YaS)

Table 5. EMMA results for all Langtang River water samples

Langtang River location	Season*	Date	$\delta^{18}O$ value	Reacted Water	Unreacted water	Monsoon-influenced
R1	EM12	11-May-12	-13.19	**24%**	**12%**	**64%**
R4	EM12	10-May-12	-13.77	**40%**	**24%**	**35%**
R5	EM12	10-May-12	-14.43	**46%**	**16%**	**37%**
R5	EM12	8-May-12	-15.00	**59%**	**0%**	**41%**
R1	LM12	20-May-12	-11.83	**6%**	**59%**	**35%**
R1	LM12	24-May-12	-12.05	**0%**	**15%**	**85%**
R2	LM12	20-May-12	-12.14	**7%**	**57%**	**36%**
R3	LM12	21-May-12	-12.32	**7%**	**63%**	**30%**
R4	LM12	22-May-12	-12.47	**0%**	**0%**	**100%**
R5	LM12	22-May-12	-12.88	**14%**	**45%**	**40%**
R1	A13	19-Oct-13	-15.42	**19%**	**58%**	**23%**
R2	A13	19-Oct-13	-15.68	**31%**	**51%**	**17%**
R3	A13	19-Oct-13	-15.82	**28%**	**48%**	**24%**
R3	A13	20-Oct-13	-15.84	**29%**	**51%**	**20%**
R4	A13	21-Oct-13	-16.34	**49%**	**26%**	**26%**
R5	A13	21-Oct-13	-16.78	**50%**	**27%**	**23%**
R7	A13	26-Oct-13	-15.83	**34%**	**43%**	**23%**
R8	A13	27-Oct-13	-17.51	**81%**	**19%**	**0%**
R8	A13	27-Oct-13	-17.46	**80%**	**20%**	**0%**
R9	A13	27-Oct-13	-17.37	**90%**	**10%**	**0%**
R6	A13	1-Nov-13	-16.48	**73%**	**8%**	**19%**
R4	A13	5-Nov-13	-15.83	**55%**	**14%**	**31%**
R5	A13	9-Nov-13	-15.87	**57%**	**14%**	**29%**
R3	A13	11-Nov-13	-15.06	**39%**	**33%**	**28%**

Langtang River location	Season*	Date	$\delta^{18}O$ value	Reacted Water	Unreacted water	Monsoon-influenced
R3	A13	12-Nov-13	-14.97	**39%**	**33%**	**29%**
R2	A13	21-Nov-13	-14.72	**29%**	**38%**	**33%**
R3	A13	21-Nov-13	-15.05	**31%**	**0%**	**69%**
R4	A13	24-Nov-13	-15.56	**54%**	**13%**	**33%**
R1	A13	25-Nov-13	-13.11	**21%**	**43%**	**36%**
R2	A13	25-Nov-13	-14.72	**29%**	**39%**	**33%**
R3	A13	25-Nov-13	-15.02	**36%**	**33%**	**31%**
R1	N08	23-Nov-08	-12.83	**15%**	**7%**	**78%**
R2	N08	24-Nov-08	-13.3	**17%**	**16%**	**67%**
R3	N08	25-Nov-08	-14	**25%**	**22%**	**54%**
Between R3 and R4	N08	25-Nov-08	-13.66	**25%**	**0%**	**75%**
R5	N08	27-Nov-08	-14.64	**43%**	**0%**	**57%**

*EM12 = Early May 2012, LM12 = Late May 2012, A13 = October/November 2013, N08 = November 2008

unconsolidated moraines and fans in the glaciated terrain. The potential storage for a large volume of groundwater in the Upper Basin would be influenced in the summer season by input of new precipitation. A combination of new precipitation and changes in snow and ice melt shift the Langtang River system away from the strong influence of reacted waters in the Early May 2012 samples, and towards unreacted water and monsoon-influence groundwater prevalence in the Late May 2012 samples.

The EMMA solutions were evaluated by reproducing concentrations of all conservative tracers from the EMMA model and comparing them to the measured values, following the protocol in Williams et al. (2006). In general, EMMA reproduced the measured concentrations well. For example, the R^2 values for magnesium, chloride, and sulfate were all greater than 0.90 with slopes near one (Figure 18). The Pearson correlation coefficient was greater than 0.92 for five tracers, and greater than 0.79 for all seven tracers, agreements comparable to those found by Liu et al. (2004) in a snowmelt dominated alpine catchment. The difference of the means was less than 12% for all tracers.

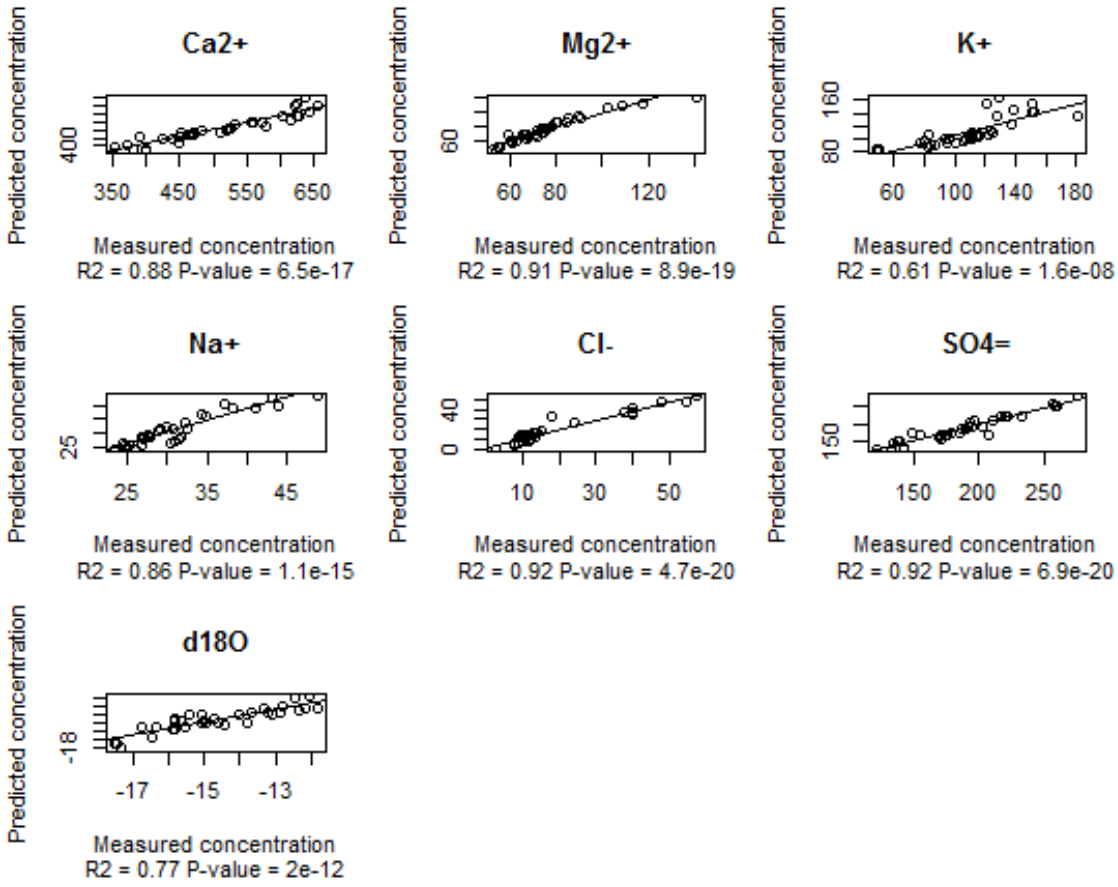

Figure 18. Tracer concentrations (µeq l-1) predicted using two Principal Components versus tracer concentrations measured in each Langtang River sample

A biplot of the principal components provides additional information on the tracers (Figure 19). The biplot indicates that variance in $\delta^{18}O$ values is explained by the first principal component and is independent of the geochemical tracers. The geochemical weathering tracers (calcium, magnesium, and sulfate) are correlated, as they all plot pointing southeast. In contrast, sodium and chloride plot to the southwest and most likely indicate that precipitation is the primary source of these solutes. These two sets of tracers help differentiate reacted and unreacted waters. Potassium is correlated with sodium and chloride, but is known to be influenced by biological controls (Likens et al., 1994) and has the lowest correlation coefficient of all the tracers. The fact that the

geochemical and precipitation tracers in the biplot both plot diagonally to the first and second axes suggests that there is a third PCA axis that would be helpful in interpreting these results, consistent with the two axes explaining only 84% of the variance.

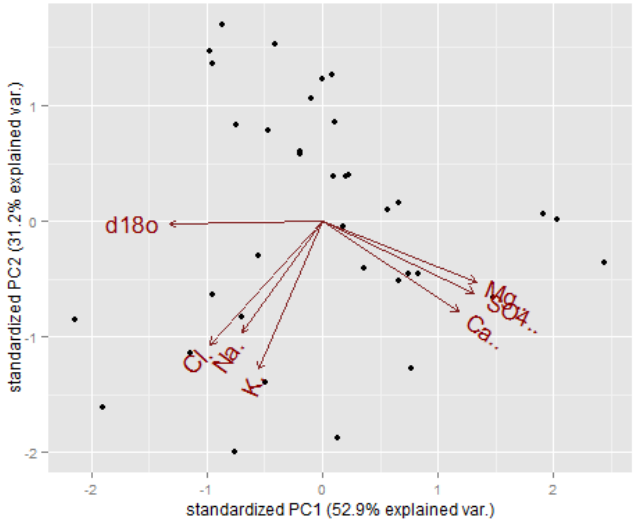

Figure 19. Biplot of Principal Component 1 and Principal Component 2

Further partitioning of the end members into rain-sourced or snow-sourced, and into snowmelt-sourced versus glacier-melt sourced, may be possible with improved spatial and temporal characterization of end member chemistry. The small sample size of rain and snow presented here does show differences between the two in most geochemical tracers and in $\delta^{18}O$ values, but a more robust data set is required to pursue this question.

With available data, EMMA estimates of unreacted, reacted, and monsoon-influenced contributions to discharge offer a plausible framework for seasonal shifts in the hydrology of the Langtang River Basin, however results for individual samples must be considered in light of limitations. Variability in end member composition, the spatial and temporal constraints on our characterization of end members, and the selection of a hypothetical monsoon-influenced end member in the analysis reduce confidence in the hydrograph separation results. Also confounding the mixing model estimates is the complexity in timing of the three end members. They are all

dependent on meteorological conditions – precipitation, temperature, and radiation - and response time to changing weather may be rapid. A more robust consideration of meteorological conditions may help explain the range of estimates of unreacted and monsoon-influenced end members. Neither river water nor end members from the monsoon are characterized here but further investigation of hydrochemistry in the summer season is warranted.

5. Conclusions

Bi-hourly, diurnal sampling of outflow from the clean-ice Khimsung Glacier and debris-covered Lirung Glacier in Early May 2012 showed a snowmelt-driven response in the Khimsung Glacier chemographs. Chemographs of Lirung Glacier outflow had a muted response which is attributed to the outflow being comprised of englacial storage with limited influence from snowmelt. Lirung outflow was strongly affected by the debris cover, which elevated geochemical solute concentrations above those of clean-ice glaciers and demonstrated the differences between reacted meltwater and unreacted meltwater explored further in the EMMA analysis. Enriched $\delta^{18}O$ values in the Lirung Glacier outflow relative to the Khimsung Glacier outflow were attributed to melt-freeze cycles driven by energy balance dynamics of the debris cover. Monsoon-season precipitation did not change the chemistry of Khimsung or Lirung Glacier outflow between pre-monsoon May 2012 samples and post-monsoon October/November 2013 samples, implying similar flow paths and residence times.

Two-component mixing model results for Langtang River water in November 2008 (reported in Racoviteanu et al., 2013), and October 2013, with $\delta^{18}O$ values as the sole tracer, produced plausible results using groundwater and meltwater end members. May 2012 river samples, however, had $\delta^{18}O$ values too enriched to be explained by groundwater and meltwater, and we found that pre-monsoon snow and rain did a better job of producing realistic results. In all

cases, meltwater contribution estimates are positively correlated with elevation, making isotopic-based mixing models a useful first cut at hydrograph separation. The inability of the two-component mixing model to consider melt water, groundwater, and snow/ice simultaneously led us to the more robust approach of EMMA.

The three-component EMMA results support the two-component results in making apparent that sub-surface flow paths and groundwater storage play a role in the hydrology of glacierized catchments that is often ignored. The presence of debris or the flow of water through moraines gives end members a reacted geochemical profile. Many of the reacted and unreacted end members defined here are influenced by melt processes, making separation of rain inputs from snow inputs difficult. Additionally, utilizing geochemical tracers instead of just isotopes allowed for the consideration of meltwater flow paths – differentiating between reacted meltwater and unreacted meltwater.

EMMA results support a conceptual model of the Langtang River basin where reacted water contributions were low and monsoon-influenced water was prominent in discharge in Late May 2012 and November 2008, relative to the shoulder seasons of the monsoon - early summer and late fall. Late fall estimates for October/November 2013 samples attributed less than a third of discharge to monsoon-influence as the system transitions towards reacted meltwater baseflow late in the year. Since the summer monsoon dominates the influx of water into the catchment and the glaciated upper basin has high porosity, groundwater storage and residence time plays an important role in the hydrology of the catchment. Understanding groundwater dynamics deserves additional attention in work examining the hydrology of high-alpine catchments in High-Mountain Asia. The isotopic gradient of monsoon precipitation we have established here is an important step towards improving quantification and understanding of both groundwater and precipitation,

rather than just snow and glacier melt processes. Further characterization of surface waters and precipitation chemistry during the monsoon and further applications of EMMA may offer additional insight into the source waters and flow paths that control Langtang River discharge.

References

Ageta, Y., and K. Higuchi. "Estimation of mass balance components of a summer-accumulation type glacier in the Nepal Himalaya." Geografiska Annaler. Series A. Physical Geography (1984): 249-255.

Anderson, Suzanne Prestrud, Sharon A. Longacre, and Erin R. Kraal. "Patterns of water chemistry and discharge in the glacier-fed Kennicott River, Alaska: evidence for subglacial water storage cycles." Chemical Geology 202.3 (2003): 297-312.

Armstrong, R.L. (2011). Establishing a collaborative effort to assess the role of glaciers and seasonal snow cover in the hydrology of the mountains of High Asia. Final Technical Proposal to USAID Solicitation No. SOL-OAA-11-000104, September 2011, 20 p.

Arnórsson, Stefán. "The use of mixing models and chemical geothermometers for estimating underground temperatures in geothermal systems." Journal of Volcanology and Geothermal Research 23.3 (1985): 299-335.

Bandyopadhyay, J., et al. "Highland waters—a resource of global significance."Mountains of the world—a global priority. The Parthenon Publishing Group(1997): 131-155.

Baral, Prashant, et al. "Preliminary results of mass-balance observations of Yala Glacier and analysis of temperature and precipitation gradients in Langtang Valley, Nepal." Annals of Glaciology 55.66 (2014): 9.

Barnard, Patrick L., et al. "Landscape response to deglaciation in a high relief, monsoon-influenced alpine environment, Langtang Himal, Nepal." Quaternary Science Reviews 25.17 (2006): 2162-2176.

Barnett, Tim P., Jennifer C. Adam, and Dennis P. Lettenmaier. "Potential impacts of a warming climate on water availability in snow-dominated regions."Nature 438.7066 (2005): 303-309.

Barthold, Frauke K., et al. "Identification of geographic runoff sources in a data sparse region: hydrological processes and the limitations of tracer-based approaches." Hydrological processes 24.16 (2010): 2313-2327.

Blasch, Kyle W., and Jeannie R. Bryson. "Distinguishing sources of ground water recharge by using δ2H and δ18O." Ground water 45.3 (2007): 294-308.

Bolch, T., et al. "The state and fate of Himalayan glaciers." Science 336.6079 (2012): 310-314.

Bookhagen, Bodo, and Douglas W. Burbank. "Toward a complete Himalayan hydrological budget: Spatiotemporal distribution of snowmelt and rainfall and their impact on river discharge." Journal of Geophysical Research: Earth Surface (2003–2012) 115.F3 (2010).

Bowen, Gabriel J., and Bruce Wilkinson. "Spatial distribution of δ18O in meteoric precipitation." Geology 30, no. 4 (2002): 315-318.

Buttle, J. M. "Isotope hydrograph separations and rapid delivery of pre-event water from drainage basins." Progress in Physical Geography 18.1 (1994): 16-41.

Chalise, Suresh R., et al. "Management of water resources and low flow estimation for the Himalayan basins of Nepal." Journal of Hydrology 282.1 (2003): 25-35.

Christophersen, Nils, et al. "Modelling streamwater chemistry as a mixture of soilwater end-members—A step towards second-generation acidification models." Journal of Hydrology 116.1 (1990): 307-320.

Christophersen, Nils, and Richard P. Hooper. "Multivariate analysis of stream water chemical data: The use of principal components analysis for the end-member mixing problem." Water Resources Research 28.1 (1992): 99-107.

Craig, Harmon. "Isotopic variations in meteoric waters." Science 133.3465 (1961): 1702-1703.

Dansgaard, Willi. "Stable isotopes in precipitation." Tellus 16.4 (1964): 436-468.

Durand, P., and J. L. Juan Torres. "Solute transfer in agricultural catchments: the interest and limits of mixing models." Journal of Hydrology 181.1 (1996): 1-22.

Fujita K, Sakai A, Chhetri TB. "Meteorological observation in Langtang Valley, 1996." Bulletin of Glacier Research 15 (1997): 71-78.

Fujita, Koji, and Takayuki Nuimura. "Spatially heterogeneous wastage of Himalayan glaciers." Proceedings of the National Academy of Sciences 108.34 (2011): 14011-14014.

Fukushima Y, Kawashima K, Suzuki M, Ohta T, Motoyama H, Kubota H, Bajracharya OR "The hydrological data of Langtang Valley, Nepal Himalayas." Bulletin of Glacier Research 5 (1987): 115-120.

Giggenbach, W. F., et al. "Isotopic and chemical composition of Parbati valley geothermal discharges, north-west Himalaya, India." Geothermics 12.2 (1983): 199-222.

Higuchi, K. "Nepal-Japan Cooperation in Research on Glaciers and Climates of the Nepal Himalaya." Snow and Glacier Hydrology (Proceedings of the Kathmandu Symposium, November 1992). IAHS Publication 218 (1993).

Hodson, Andy, et al. "Chemical denudation and silicate weathering in Himalayan glacier basins: Batura Glacier, Pakistan." Journal of hydrology 262.1 (2002): 193-208.

Hoeg, S., S. Uhlenbrook, and Ch Leibundgut. "Hydrograph separation in a mountainous catchment—combining hydrochemical and isotopic tracers."Hydrological Processes 14.7 (2000): 1199-1216.

Hooper, Richard P., and Christine A. Shoemaker. "A comparison of chemical and isotopic hydrograph separation." Water Resources Research 22.10 (1986): 1444-1454.

Hooper, Richard P., Nils Christophersen, and Norman E. Peters. "Modelling streamwater chemistry as a mixture of soilwater end-members—An application to the Panola Mountain catchment, Georgia, USA." Journal of Hydrology 116.1 (1990): 321-343.

Hooper, Richard P. "Diagnostic tools for mixing models of stream water chemistry." Water Resources Research 39.3 (2003).

Immerzeel, Walter W., Ludovicus PH van Beek, and Marc FP Bierkens. "Climate change will affect the Asian water towers." Science 328.5984 (2010): 1382-1385.

Immerzeel, Walter W., et al. "Hydrological response to climate change in a glacierized catchment in the Himalayas." Climatic Change 110.3-4 (2012): 721-736.

Immerzeel, W. W., et al. "The importance of observed gradients of air temperature and precipitation for modeling runoff from a glacierized watershed in the Nepalese Himalayas." Water Resources Research 50.3 (2014): 2212-2226.

Johnsen, S. J., W. Dansgaard, and J. W. C. White. "The origin of Arctic precipitation under present and glacial conditions." Tellus B 41.4 (1989): 452-468.

Junge, Christian E., and R. T. Werby. "The concentration of chloride, sodium, potassium, calcium, and sulfate in rain water over the United States." Journal of Meteorology 15.5 (1958): 417-425.

Kansakar, Sunil R., et al. "Spatial pattern in the precipitation regime of Nepal."International Journal of Climatology 24.13 (2004): 1645-1659.

Kargel, Jeffrey S., et al. "Himalayan glaciers: The big picture is a montage."Proceedings of the National Academy of Sciences 108.36 (2011): 14709-14710.

Karim, Ajaz, and Jan Veizer. "Water balance of the Indus River Basin and moisture source in the Karakoram and western Himalayas: Implications from hydrogen and oxygen isotopes in river water." Journal of Geophysical Research: Atmospheres (1984–2012) 107.D18 (2002): ACH-9.

Kaser, Georg, Martin Großhauser, and Ben Marzeion. "Contribution potential of glaciers to water availability in different climate regimes." Proceedings of the National Academy of Sciences 107.47 (2010): 20223-20227.

Kaufmann, Viktor, et al. "Digital Camera Nikon D300 in Support of High Mountain Studies in the Langtang Valley, Central Himalaya, Nepal." (2013).

Kayastha, Rijan Bhakta, et al. "Practical prediction of ice melting beneath various thickness of debris cover on Khumbu Glacier, Nepal, using a positive degree-day factor." IAHS PUBLICATION (2000): 71-82.

Kayastha RB, Ageta Y, Nakawo M, Fujita K, Sakai A, Matsuda Y. "Positive degree-day factors for ice ablation on four glaciers in the Nepalese Himalayas and Qinghai-Tibetan Plateau." Bulletin of Glaciological Research 20 (2003): 7-14.

Kong, Yanlong, and Zhonghe Pang. "Evaluating the sensitivity of glacier rivers to climate change based on hydrograph separation of discharge." Journal of Hydrology 434 (2012): 121-129.

Lambs, Luc. "Correlation of conductivity and stable isotope 18O for the assessment of water origin in river system." Chemical Geology 164.1 (2000): 161-170.

Likens, Gene E., et al. "The biogeochemistry of potassium at Hubbard Brook."Biogeochemistry 25.2 (1994): 61-125.

Liu, Fengjing, Mark W. Williams, and Nel Caine. "Source waters and flow paths in an alpine catchment, Colorado Front Range, United States." Water Resources Research 40.9 (2004).

Liu, Fengjing. https://www.eng.ucmerced.edu/people/rbales/Courses/ES214files/Emma_Liu (undated).

Marinoni, A., et al. "Chemical composition of freshsnow samples from the southern slope of Mt. Everest region (Khumbu-Himal region, Nepal)."Atmospheric Environment 35.18 (2001): 3183-3190.

Maurya, A. S., et al. "Hydrograph separation and precipitation source identification using stable water isotopes and conductivity: River Ganga at Himalayan foothills." Hydrological Processes 25.10 (2011): 1521-1530.

Messerli, Bruno, Daniel Viviroli, and Rolf Weingartner. "Mountains of the world: vulnerable water towers for the 21st century." Ambio (2004): 29-34.

Miller, James D., Walter W. Immerzeel, and Gwyn Rees. "Climate change impacts on glacier hydrology and river discharge in the Hindu Kush-Himalayas: a synthesis of the scientific basis." Mountain Research and Development 32.4 (2012): 461-467.

Motoyama, H., and T. Yamada. "Hydrological observations of langtang Valley, Nepal Himalayas during 1987 monsoon− postmonsoon season." Bulletin of glacier research 7 (1989): 195-201.

Nakawo, Masayoshi, and Birbal Rana. "Estimate of ablation rate of glacier ice under a supraglacial debris layer." Geografiska Annaler: Series A, Physical Geography 81.4 (1999): 695-701.

Neal, Colin, et al. "Declines in phosphorus concentration in the upper River Thames (UK): Links to sewage effluent cleanup and extended end-member mixing analysis." Science of the total environment 408.6 (2010): 1315-1330.

Nepal, S., et al. "Understanding the hydrological system dynamics of a glaciated alpine catchment in the Himalayan region using the J2000 hydrological model." Hydrological Processes 28.3 (2014): 1329-1344.

Poage, Michael A., & C. Page Chamberlain. "Empirical relationships between elevation and the stable isotope composition of precipitation and surface waters: considerations for studies of paleoelevation change." American Journal of Science 301.1 (2001): 1-15.

Racoviteanu, Adina E., Richard Armstrong, and Mark W. Williams. "Evaluation of an ice ablation model to estimate the contribution of melting glacier ice to annual discharge in the Nepal Himalaya." Water Resources Research 49.9 (2013): 5117-5133.

Robson, Alice, and Colin Neal. "Hydrograph separation using chemical techniques: an application to catchments in mid-Wales." Journal of Hydrology116.1 (1990): 345-363.

Sakai, Akiko, Masayoshi Nakawo, and Koji Fujita. "Melt rate of ice cliffs on the Lirung Glacier, Nepal Himalayas, 1996." Bull. Glacier Res 16 (1998): 57-66.

Sakai A, Fujita K, Aoki T, Asahi K, Nakawo M. “Water discharge from the Lirung Glacier in Langtang Valley, Nepal Himalayas, 1996.” Bulletin of Glacier Research 15 (1997): 79-83.

Seko K, Takahashi S. “Characteristics of winter precipitation and its effect on glaciers in the Nepal Himalaya.” Bulletin of Glacier Research 9 (1991): 9-16.

Shimabukuro, Yosio Edemir, and A. Smith. "The least-squares mixing models to generate fraction images derived from remote sensing multispectral data."Geoscience and Remote Sensing, IEEE Transactions on 29.1 (1991): 16-20.

Shiraiwa T, Ueno K, Yamada T. “Distribution of mass input on glaciers in the Langtang Valley, Nepal Himalayas.” Bulletin of Glacier Research 10 (1992): 21-30

Sklash, M. G., R. N. Farvolden, and P. Fritz. "A conceptual model of watershed response to rainfall, developed through the use of oxygen-18 as a natural tracer." Canadian Journal of Earth Sciences 13.2 (1976): 271-283.

Steig, Eric J., et al. "The geochemical record in rock glaciers." Geografiska Annaler: Series A, Physical Geography 80.3-4 (1998): 277-286.

Sueker, Julie K., et al. "Effect of basin physical characteristics on solute fluxes in nine alpine/subalpine basins, Colorado, USA." Hydrological pro

Takahashi S, Motoyama H, Kawashima K, Morinaga Y, Seko K, Iida H, Kubota H, Turadahr NR. "Summary of meteorological data at Kyangchen in Langtang Valley, Nepal Himalayas, 1985-1986." Bulletin of Glacier Research 5 (1987): 121-128

Taylor, Susan, et al. "How isotopic fractionation of snowmelt affects hydrograph separation." Hydrological Processes 16.18 (2002): 3683-3690.

Thapa, K. B. "Estimation of snowmelt runoff in Himalayan catchments incorporating remote sensing data." IAHS Publications-Publications of the International Association of Hydrological Sciences 218 (1993): 69-74.

Thompson, Lonnie G., et al. "A high-resolution millennial record of the South Asian monsoon from Himalayan ice cores." Science 289.5486 (2000): 1916-1919.

U.N. Environmental Program and World Glacier Monitoring Service, Global Glacier Change: Facts and Figures UNEP Publ., http://www.grid.unep.ch/glaciers/ (2008): Section 6.9: Regional Glacier Changes in Central Asia.

Vaughn, B. H. Stable Isotopes as Hydrologic Tracers in South Cascade Glacier. Boulder, University of Colorado. Masters Thesis (1994), 143 p.

Wagnon, Patrick, et al. "Four years of mass balance on Chhota Shigri Glacier, Himachal Pradesh, India, a new benchmark glacier in the western Himalaya." Journal of Glaciology 53.183 (2007): 603-611.

Wake, Cameron P., et al. "The chemical composition of aerosols over the eastern Himalayas and Tibetan Plateau during low dust periods." Atmospheric Environment 28.4 (1994): 695-704.

Wels, Christoph, R. Jack Cornett, and Bruce D. Lazerte. "Hydrograph separation: A comparison of geochemical and isotopic tracers." Journal of Hydrology 122.1 (1991): 253-274.

Williams, M. W., et al. "Geochemistry and source waters of rock glacier outflow, Colorado Front Range." Permafrost and Periglacial Processes 17.1 (2006): 13-33.

Williams, Mark W., Christine Seibold, and Kurt Chowanski. "Storage and release of solutes from a subalpine seasonal snowpack: soil and stream water response, Niwot Ridge, Colorado." Biogeochemistry 95.1 (2009): 77-94.

Williams, Mark W., et al. "Stream water chemistry along an elevational gradient from the Continental Divide to the foothills of the Rocky Mountains." Vadose Zone Journal 10.3 (2011): 900-914.

Xu, Jianchu, et al. "The melting Himalayas: cascading effects of climate change on water, biodiversity, and livelihoods." Conservation Biology 23.3 (2009): 520-530.

Yamdata T, Shiraiwa T, Iida H, Kadota T, Watanabe T, Rana B, Ageta Y, Fushimi H. “Fluctuations of the glaciers from the 1970s to 1989 in the Khumbu, Shorong and Langtang regions, Nepal Himalayas.” Bulletin of Glacier Research 10 (1992): 11-19.

Yoshimura Y, Kohshima S, Takeuchi N, Seko K, Fujita K. “Snow algae in a Himalayan ice core: new environmental markers for ice core analyses and their correlation with summer mass balance.” Annals of Glaciology 43 (2006): 148-153.

Zemp, M., M. Hoelzle, and W. Haeberli. "Six decades of glacier mass-balance observations: a review of the worldwide monitoring network." Annals of Glaciology 50.50 (2009): 101-111.

Zhang, Xinping, et al. "Variation of precipitation δ18O in Langtang Valley Himalayas." Science in China Series D: Earth Sciences 44.9 (2001): 769-778

Appendix 1: Protocols for surface water sampling

General Sampling Notes:

- Filters may be re-used multiple times if you are collecting the same type of sample (e.g. all rain samples).
- If you switch from a 'dirtier' sample (e.g. river water) to a 'cleaner' sample (e.g. rain or spring water), you must change the filter and rinse the filter holder as best as possible.
- Avoid all contact between your hands and things which are in direct contact with the sample (e.g. filters, syringe tip, etc.).
- Never pull water backwards through the filter (from bottom to top) – this will tear the filter.

1. Supplies

A) New 125mL or 250mL Nalgene HDPE (high-density polyethylene) bottles with lids (or similar) for major chemistry analysis (anions, cations)
B) 25mL glass vials for isotope samples
C) 1.0-um 47 mm binder free, glass fiber Millipore filters
D) Millipore reusable 47 mm inline filter holder

E) Tweezers for handling filters.
F) 60 mL sterile syringes
G) Labeling tape
H) Sharpie marker for labeling
I) Sample dipper - an open container to hold water: plastic cup or bottom half of water bottle (ideally it will hold several hundred mm of water)

2. Bottles and Labeling System

A) Label the bottle before collecting sample
B) Labeling tape should be wrapped around the entire circumference of the plastic bottle
-if the label is not waterproof, cover it completely (after writing the sample name) by wrapping clear tape around the circumference of the bottle
C) Location codes should uniquely describe location. GPS coordinates for all locations should be known. For locations sampled previously, use same name (if known).
D) For samples coming to Colorado, label the bottle with a Sample ID as follows:

Format: Location Code-YYYYMMDD-TIME
Example: LAMA-20120630-1345
Example: Spring at Rimpoche-20120630-1725

3. Filtration Technique

A) Rinse your hands with stream water and shake dry or dry with clean cloth
B) Rinse the sample dipper with sample water 3 times

C) Open plastic filter holder and remove old filter paper from filter holder if present
D) The piece with the Millipore label is the top half
E) If possible, rinse filter holder with sample water by submerging it in surface water that has been collected in the dipper
F) Ensure the two O-rings stay secured, one on the bottom half, one on the top half.

* Top piece is on right. The O-rings should remain on the filter holder while you replace the filter. There is no need to set them on another surface that is potentially contaminated.

G) Use tweezers (dipped in water and shaken dry or wiped with clean cloth) to insert new filter paper with the rough/uneven side facing down

H) Put the 2 pieces of the filter holder back together. Make sure O-rings stay in place.
I) Use the sample dipper to collect new water from the stream
J) Pour this water over the outside of the syringe to rinse off any dust
K) Dip more water from the stream as needed for the following steps
L) Use the syringe to pull ~30mL of water out of the dipper
M) Pull the plunger as far back as possible without removing it, allowing the water to rinse the entire 60mL volume of the syringe

N) Turn the syringe upside down and shake the water around to clean the syringe
O) NEVER TOUCH THE TIP OF THE SYRINGE WITH YOUR FINGERS
P) Discard water from the syringe onto ground
Q) Repeat steps M through P twice (x2) for a total of 3 rinses
R) Open the sample bottle (100mL or 250mL) – it will be rinsed 3 times with 30mL of filtered sample
S) Pull 60mL of water into the syringe
T) Turn the syringe upside down and push the plunger forward until all air has been removed
U) Attach the syringe to the filter holder

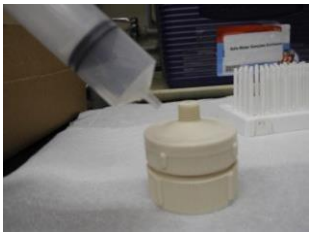

V) Push 30mL of water through the filter and into the sample bottle

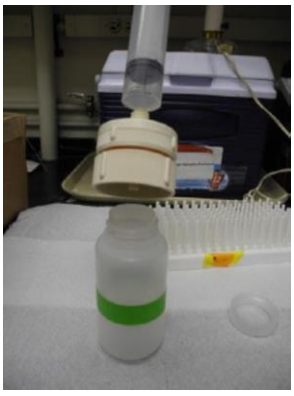

W) Put the cap on the bottle and shake to rinse
X) Discard the water
Y) Push the next 30mL of water through the filter and into the sample bottle
Z) Again, close the bottle, shake, and discard
AA) Detach the syringe from the filter holder and pull another 30mL of water into the syringe – this is the 3rd and final 30mL rinse

BB) Attach the syringe to the filter holder and push through filter and into bottle for final rinse. Shake and discard as before

CC) Refill the sample dipper as needed

DD) Pull water into syringe and filter into the bottle until it is full, being careful not to let the tip of the filter holder touch the water in the bottle

EE) Close the bottle tightly

FF) Document the day, time and GPS location of the sample, and take a photo

GG) Store bottle out of sunlight, at 4oC (or as cold as possible). Freezing is also an option - in this case the bottles should have some air left at the top so the water can expand.

Appendix 2: Protocols for construction of bulk precipitation samplers

The purpose of each plastic bucket and funnel is to collect rain (or snow) for chemical isotope analysis (Oxygen-18 and Deuterium (Hydrogen-2)) and other chemistry data. Understanding how the chemistry of precipitation changes with elevation and how it changes over time is an important parameter for estimating source contributions to streamflow through End Member Mixing Analysis (EMMA).

Note: All parts of the precipitation samplers - buckets (15 liters or 17 liters), lids and funnels - should be kept well-sealed during travel to prevent contamination from dust.

Supplies

1. Plastic buckets, 15 or 17 liter volume
2. Lids for all buckets
3. Plastic funnels for each bucket (approximately 9cm in diameter, a long neck helps stabilize it inside the bucket)

4. Mesh wire (for example: metal window screening, below) – enough to cut and cover all funnels. It should be flexible enough that you are able to cut it and bend it over the funnel.

5. Polyester fiber to filter dust (a small piece for each funnel)

6. Mineral oil (Johnson's Baby Oil, below) to serve as evaporation barrier – each bucket needs approximately 150mL of new oil each time it is sampled. More Baby Oil can be sent later if needed.

Construction of buckets

a. Insert funnel into lid (secured with tape or silicone sealant)
b. Cover funnel with mesh (mesh secured with zip ties)
c. Additional zip ties attached, pointing straight up to deter birds from landing

d. Wrap all components (buckets separated from lids with funnels) in plastic bags to ensure no contamination from dust while in transit to the field.
e. IN THE FIELD: ad Baby Oil, attach lid. For field sampling, use 'Protocols for Water Sampling'.

Establishing a 'control sample':

A control sample will be used to quantify how the oil (used to prevent evaporation) mixes with the water sample. This requires a bucket with tap water and oil with a lid being placed next to one of the precipitation sampling buckets. The control sample will **not** have a funnel to collect rain.

When the rain samples are collected from the funnel buckets, a sample will also be collected from the control bucket to see how the water and oil have mixed. This will represent contamination of the rain samples by the oil.

a. There only needs to be one control bucket – you can put it wherever is easiest
b. The control bucket can be smaller than the sampling buckets. I have used an 8 liter bucket in the past. The only requirement is that it has a tight-fitting lid.
c. Make a ~1cm hole on the side of the bucket near the top to provide ventilation
d. From a sink or other tap water source, use the sample dipper (plastic cup) to collect a filtered sample using the protocols below (Protocols for surface water sampling)
e. Add oil to the bucket to a depth of ~1cm
f. Measure the depth of the oil
g. Fill the bucket 10 - 15cm deep with tap water
h. Secure the lid on the bucket and stabilize with rocks
i. Document the date, time and take a photo of the bucket
j. When sampling bulk precipitation collectors next time, also collect a sample from the control bucket.

Installation of new bulk precipitation samplers:

a. Unwrap bucket, lid and funnel from their protective packaging
b. Add oil to a depth of approximately 1cm
c. Measure the depth of the oil layer (if possible)
d. Put the lid on and secure however possible (e.g. duct tape)
e. Stack rocks around the bucket for stabilization
f. Document the day and time of installation and any problems you had
g. Take GPS coordinates of bucket's location
h. Take a photo of the bucket

Appendix 3: Protocols for sample extraction from bulk precipitation buckets

General Sampling Notes: Filters may be re-used multiple times if you are collecting the same type of sample (e.g. all rain samples). If you switch from a 'dirtier' sample (e.g. river water) to a 'cleaner' sample (e.g. snow melt or spring water), you must change the filter and rinse the filter holder as well as possible. Also, avoid all contact between your hands and things which are in direct contact with the sample (e.g. filters, syringe tip, etc.). Never pull water backwards through the filter (from bottom to top) – this can tear the filter.

*Note that for isotope sampling, samples do not need to be filtered. However it is useful to also analyze precipitation samples for major chemistry and this requires filtering. The absolute minimum volume for major chemistry is 50mL (2 glass bottles), but it is safer to collect a larger volume (e.g. 100mL).

1.) Supplies

A) Clean 25mL clear glass bottles (100mL plastic bottles are also fine)

B) 1.0-um 47 mm binder free, glass fiber Millipore filters for non-low ionic concentration water samples, or Whatman GF/C 1.2 µm glass micro-fiber filters; with Millipore reusable 47 mm inline filter holder

C) Tweezers for handling filters.

D) 60 mL sterile syringes.

E) Labeling tape

F) Sharpie marker for labeling

2.) Bottles and Labeling System

A) Labeling tape should be wrapped around the entire circumference of the plastic bottle
-if the label is not waterproof, cover it completely by wrapping clear tape around the circumference of the bottle

B) Location codes should be 3-4 letters, and GPS coordinates for the location should be known

C) For samples coming to Colorado, label the bottle with a Sample ID as follows:
Location Code-BULKPCP-DDMMYY-TIME
Example: LAMA-BULKPCP-300612-1345

3.) Filtration Technique

A) Make sure your hands are clean – wash if possible and wipe dry with clean cloth

B) If possible, rinse filter with sample water

C) Open the plastic filter holder. The threaded piece with Millipore label is the top half.

D) Ensure the two O-rings stay secured, one on the bottom half, one on the top half.

*The O-rings should remain on the filter holder while you replace the filter. There is no need to set them on another surface that is potentially contaminated

E) Remove the old filter paper

F) Use tweezers (wiped dry with clean cloth) to insert new filter paper with the rough/uneven side facing down

G) Put the 2 pieces of the filter holder back together. Make sure O-rings stay in place.

H) Remove lid of bucket

I) Estimate the depth of liquid to determine whether there is sufficient water for a sample (25mL) and rinsing of syringe and filter (90mL).

-If liquid is not deep enough, tilt the bucket and allow several minutes for the oil to separate, and then try to extract a sample

J) Wipe the outside of the syringe with a clean cloth to remove dust

K) Insert the syringe into the water, deep enough that none of the 1cm layer of oil is removed.

L) Draw 30mL of sample water into the syringe

M) Pull the plunger as far back as possible without removing it, allowing the water to rinse the entire 60mL volume of the syringe

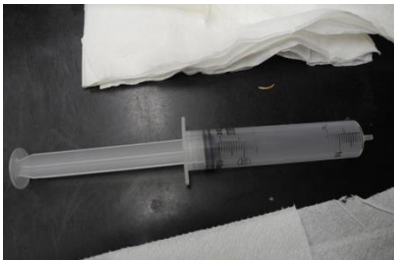

N) Turn the syringe upside down and shake the water around to clean the syringe

O) NEVER TOUCH THE TIP OF THE SYRINGE WITH YOUR FINGERS

P) Discard water from the syringe onto ground

Q) Insert the syringe through the oil and draw 60mL of sample water

R) Turn the syringe upside down and push the plunger forward until all air has been removed

S) Attach the syringe to the filter holder and push all 60mL of water through the filter to rinse the filter

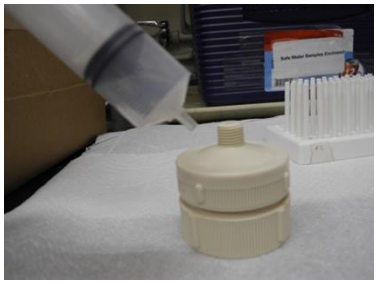

T) Detach syringe from filter

U) Wipe the outside of the syringe with a clean cloth to remove any oil

V) Insert the syringe through the oil and draw ANOTHER 60mL of sample water

W) Turn the syringe upside down and push the plunger forward until all air has been removed

X) Attach the syringe to the filter holder

Y) This time, put the filter holder over the 25mL glass sample bottle, which has already been labeled with the sample ID

Z) Fill the glass bottle to the top, without letting the filter holder touch the water in the bottle

*Note that the 25mL glass bottles are specifically for isotope analysis since they are designed to eliminate all air from the sample. If you would like to do major chemistry analysis on the precipitation sample, you will need to collect at least two 25mL bottles, or also fill a larger plastic bottle.

AA) Screw the lid on tightly and store the bottle in a safe place, out of sunlight, so it doesn't break. At 4^{o}C if possible.

BB) Document day, time, and GPS coordinates in a field notebook and take a picture!